Journal of Marine Research, 50, 1–31, 1992

Journal of
MARINE RESEARCH

Volume 50, Number 1

Integral equation approach to tropical ocean dynamics: Part I—Theory and computational methods

by Marcio L. Vianna[1] and Paulo R. Holvorcem[1,2]

ABSTRACT

In linear, three-dimensional, continuously stratified equatorial β-plane ocean models with arbitrary eastern and western boundaries the shallow water equations for each vertical mode must be solved numerically in the horizontal variables. This paper introduces a new numerical method of solution for the time-Fourier transformed shallow water equations with slip boundary conditions at boundaries of arbitrary geometry. The method is based on a boundary integral equation (BIE) for the pressure perturbation response to the specified wind-stress forcing field. All other dependent variables are expressed as boundary functionals of the pressure perturbation. The kernels of all functionals are constructed from the Green's function for the Laplace Tidal Equation on the β-plane and its derivatives. The efficient computation of these kernels from their exact meridional mode representations may be performed by use of asymptotic methods especially developed for the numerical evaluation of functions expressed as slowly converging series of Hermite functions. The solution of the basic BIE and the computation of the boundary functionals involve the discretization of the ocean boundaries into a number of boundary segments (boundary elements). It is shown that the terms of the BIE involving the wind-stress field over the ocean may be reduced to a boundary integral, which effectively reduces the simulation problem to the solution of a one-dimensional BIE. The method incorporates the ocean physics through the relationship between the coastal pressure field and the basin-wide variables, pointing out to the possibility that the dynamic topography of the ocean may be estimated directly from the wind-stress field and coastal sea-level data.

1. Divisão de Ciências da Terra, Instituto Nacional de Pesquisas Espaciais, Av. dos Astronautas 1758, São José dos Campos, SP, 12201, Brazil.

2. Present address: Instituto de Matemática, Estatística e Ciência da Computação, Universidade Estadual de Campinas, C.P. 6065, Campinas, SP, 13081, Brazil.

1. Introduction

Numerical simulations of the wind-forced tropical ocean circulation usually employ the finite-difference method to solve a set of model equations (McCreary, 1985). In linear, three-dimensional models which assume a flat bottom and a vertical stratification that does not vary horizontally, separation of variables allows the reduction of the three-dimensional problem to a series of two-dimensional problems in the horizontal variables. While finite-differencing is used in the horizontal variables, the time dependence of each of these two-dimensional problems may be dealt with either by direct time integration or by use of some integral transform (usually a Fourier or Laplace transform). When non-linear models are considered, the only practical solution method seems to be to use multi-level finite-difference schemes (Bryan, 1969). This method has been used over the years since 1980 by Philander and Pacanowski (see, e.g., Philander and Pacanowski, 1986) to discuss several features of the ocean response to a variety of wind setups, including seasonally varying and realistic winds. Although these simulations seem to be realistic, some practical limitations on its applicability to study the physics of several important phenomena can be identified:

(1) The model is very complex, in the sense that only a small group of researchers can do few numerical experiments per year, and each experiment is also computationally time-consuming.

(2) The various authors recognize that western boundary phenomena, relating the wind field to the dynamics of the North Brazil Current, which veers offshore (Bruce *et al.,* 1985) in a clear seasonal pattern, are left unexplained.

(3) The discussion of the relation between local and non-local responses in the tropical Atlantic, and the periodic versus the "initial value" (impulse) response needs more detailed support from additional specialized numerical experiments.

On the other hand, linear three-dimensional models, that in principle should be easier to apply by a large number of interested authors, have suffered from even more serious practical drawbacks. We will comment on a few representative models developed so far as illustrative examples of these drawbacks.

(a) Inability to accurately apply boundary conditions at slanted or irregular boundaries in a computationally efficient and simple way: in McCreary *et al.* (1984), the $2\Delta x$ noise introduced by the finite-difference discretization was a problem, so that a large horizontal viscosity had to be introduced. Moreover, the boundary geometries (east and west) are unrealistic. The simplicity of the linear theory is thus lost, and it would therefore be more efficient to use the finite-difference code with realistic boundaries and wind forcings for each of the baroclinic modes. In fact, the linear reduced gravity model of Busalacchi and Picaut (1983) accomplished this objective independently, and our integral equation method should be tested against some of their results. However, a large horizontal eddy viscosity was also introduced in their simulation in order to damp the short waves near the boundaries.

(b) Many authors use the long-wave approximation, which reflects the basic inability to satisfy boundary conditions at slanted boundaries with the use of the complete horizontal normal mode expansions. They also reflect computational problems with the summation of series of meridional modes (Cane and Patton, 1984; Boyd and Moore, 1986). Therefore, in these theories the true capabilities of the linear theory in explaining important phenomena, especially near western boundaries, are probably lost and have never been appreciated to date. The models of Cane and Patton (1984), Cane and Sarachik (1981) (see Cane and Sarachik, 1983, for a review) and du Penhoat and Treguier (1985) all fall in this category. The present-day recognized importance of linear theory as a valid model, rather than as a diagnostic tool, relates to its effectiveness in representing sea surface dynamic height (du Penhoat and Gouriou, 1987; Philander and Pacanowski, 1987), and the recent proof that interannual variability in tropical ocean-atmosphere models is well described by linear theory (Battisti and Hirst, 1989; Seager *et al.,* 1988; Zebiak and Cane, 1987).

With the availability of large sets of synoptic wind-stress data, to be obtained from scatterometer data from satellites to be launched in the near future, and with altimeter data already available from Geosat (Carton, 1989), the development of new computationally efficient three-dimensional linear models that include the complete meridional mode superposition and are forced by realistic winds over realistic tropical ocean geometries is of general interest. This work is devoted to the development of a practical and accurate computational method of solution of boundary value problems for the shallow water equations with slip boundary conditions at eastern and western boundaries of arbitrary shape. The analytical-numerical analysis presented here is described in the traditional language of mathematical physics. By use of a Green's function for the Laplace Tidal Equation on the β-plane (Matsuno, 1966), we display how local and non-local influences are propagated throughout the ocean basin.

We derive integral relations between the pressure and velocity perturbations over the ocean basin and the pressure distribution along the ocean boundaries. These relations involve boundary functionals of the pressure, so once the pressure distribution along the boundaries is known, one can determine at once the dependent variables in any restricted region of the ocean with whatever resolution is necessary. To accomplish this, the kernels of the boundary functionals, or "influence functions," have to be computed with the aid of new asymptotic methods which allow the efficient summation of slowly convergent series of Hermite functions (Holvorcem, 1992).

The computation of the boundary pressure distribution is performed by solving the basic boundary integral equation (BIE) of the theory (Vianna, 1988). A practical solution may be obtained by the standard boundary element method (Brebbia *et al.,* 1984). All boundary integrals appearing in the boundary integral equation may be calculated by this method. We also show how to reduce a two-dimensional domain

integral term containing the arbitrary wind-forcing field, which is usually given on a standard grid (Picaut *et al.,* 1985), to a boundary integral.

Part II of this series (Holvorcem and Vianna, 1992) presents a BIE formulation for equatorial wave scattering problems with arbitrary boundary geometry, which is derived from the theory of this paper. It also describes the first numerical experiments with the boundary element method in equatorial ocean modeling, through a study of the scattering of equatorial Rossby waves from a model equatorial Atlantic western boundary of realistic horizontal geometry. The most prominent features in the resulting interference patterns turn out to be amplitude maxima arising from the superposition of short wave modes excited at the western boundary by the incident Rossby wave. Similarities and differences between these simulations and the observed intraseasonal oscillations in the equatorial Atlantic Ocean are also discussed in Part II.

Future developments of the methodology presented in this paper will include a BIE formulation for initial-boundary value problems for the shallow water equations, thus allowing the study of the transient ocean response.

2. Model equations

The equations of motion for the horizontal structure of the baroclinic modes in a vertical mode expansion of the linear, continuously stratified β-plane model of McCreary (1981), in which the coefficients of vertical diffusion of heat and momentum are given by

$$\kappa = \nu = A/N^2(z), \tag{2.1}$$

are the shallow water equations

$$\rho_o(\partial_t \mathbf{u} + \beta y \hat{\mathbf{z}} \times \mathbf{u}) = -\nabla p - (\rho_o A/c^2)\mathbf{u} + \mathbf{F}, \tag{2.2}$$

$$\partial_t p + (A/c^2)p + \rho_o c^2 \nabla \cdot \mathbf{u} = 0. \tag{2.3}$$

In these equations, ρ_o is a scale density of water, p, $\mathbf{u}$ and $\mathbf{F}$ represent the projections of the pressure, velocity and wind-stress onto the given baroclinic mode, and c is the vertical eigenvalue of that mode.

If (2.2) and (2.3) are Fourier transformed in time, using the definition

$$f(\omega) = \int_{-\infty}^{\infty} e^{-i\omega t} f(t)\, dt, \tag{2.4}$$

then the transformed version of (2.2) may be solved for $\mathbf{u}$ in terms of p and $\mathbf{F}$:

$$\mathbf{u} = (\rho_o \beta)^{-1}(y^2 - y_c^2)^{-1}(iy_c - y\hat{\mathbf{z}} \times)(\mathbf{F} - \nabla p), \tag{2.5}$$

where

$$y_c = (\omega - i\Delta\omega)/\beta, \quad \Delta\omega = A/c^2. \tag{2.6}$$

Substituting this expression for $\mathbf{u}$ in the transformed version of (2.3), a single equation for $p = p(x, y, \omega)$ is obtained (Vianna, 1988),

$$\mathscr{L}p = S, \tag{2.7}$$

with

$$\mathscr{L} = \mathscr{L}(y_c) = \nabla \cdot [(y^2 - y_c^2)^{-1}(y\hat{\mathbf{z}} \times - iy_c)\nabla] + iy_c/4, \tag{2.8}$$

$$S = \nabla \cdot [(y^2 - y_c^2)^{-1}(y\hat{\mathbf{z}} \times - iy_c)\mathbf{F}']. \tag{2.9}$$

In (2.8) and (2.9) and in the rest of this paper the variables x, y and y_c are non-dimensionalized by the equatorial deformation radius,

$$R_o = (c/2\beta)^{1/2}; \tag{2.10}$$

we also define $\mathbf{F}' = R_o\mathbf{F}$. In non-dimensional units, the real part of y_c becomes

$$\mathrm{Re}\, y_c = \omega/\beta R_o = \omega/\omega_o, \tag{2.11}$$

which gives a non-dimensional measure of frequency, with scale $\omega_o = \beta R_o$.

Eq. (2.7) is essentially the Laplace Tidal Equation on the β-plane (Matsuno, 1966). If there is some dissipation ($A \neq 0$), its singular points at $y = \pm y_c$ will not lie on the physical range (real y). At the latitudes $y = \pm \mathrm{Re}\, y_c$, the frequency ω is equal to the local Coriolis parameter. In the next sections, we shall see that the singular points do not affect the regularity of the solutions of (2.7) for p, although they can introduce a resonance in the velocity field. This is reasonably consistent with an observation by Longuet-Higgins (1965), which states that the singularities of the Laplace Tidal Equation are "removable."

Since the model is horizontally inviscid, the boundary conditions must specify the normal flow through the boundary Γ of the oceanic region B over which we want to solve the shallow water equations. In the time domain, such a boundary condition is

$$\mathbf{u} \cdot \hat{\mathbf{n}} = q(s, t) \tag{2.12}$$

on Γ, where $\hat{\mathbf{n}}$ is the outer normal vector to Γ, and q is a given function of time and the coordinate s, which measures length along Γ. When $q = 0$, we have the usual slip condition to be applied at rigid boundaries. A situation where $q \neq 0$ can represent, for example, a prescribed river discharge at a continental margin. Taking the scalar product of (2.5) with $\hat{\mathbf{n}}$, one obtains an equivalent form of (2.12) in terms of the pressure perturbation p,

$$(y^2 - y_c^2)^{-1}(iy_c\hat{\mathbf{n}} + y\hat{\mathbf{s}}) \cdot (\mathbf{F}' - \nabla p) = \tfrac{1}{2}\rho_o c q(s, \omega) \tag{2.13}$$

on Γ, where $\hat{\mathbf{s}} = \hat{\mathbf{z}} \times \hat{\mathbf{n}}$ is the counterclockwise tangent vector to Γ and $q(s, \omega)$ denotes the Fourier transform of $q(s, t)$. This is the boundary condition that must be applied to the governing equation (2.7) for the pressure perturbation field.

3. Integral relations and influence functions

To be able to express (2.7) and (2.13) as a Boundary Integral Equation (BIE), we derive an integral theorem for the operator $\mathscr{L}(y_c)$ which corresponds to Green's theorem of vector calculus (Hildebrand, 1965). Green's theorem involves an inner product in the linear function space of complex-valued functions defined over an ocean region B. We define the inner product of two complex functions of the position vector $\mathbf{r} = (x, y)$ by

$$\langle f, g \rangle = \iint_B f g^* \, dx \, dy, \tag{3.1}$$

where the star denotes the complex conjugate. Most authors in boundary element research (Brebbia *et al.*, 1984) define their inner products without the complex conjugate in (3.1), even when working with complex-valued functions like $p(x, y, \omega)$. We adopt the definition (3.1), which is the standard one for use with complex vector spaces (Friedman, 1956). By using (3.1), we can calculate $\langle \mathscr{L}(y_c) f, g \rangle$. Integrating by parts twice, and using the divergence theorem, we get the following identity:

$$\begin{aligned} \langle \mathscr{L}(y_c) f, g \rangle + \langle f, \mathscr{L}(y_c^*) g \rangle = \oint_\Gamma (y^2 - y_c^2)^{-1} [& f (i y_c \hat{\mathbf{n}} - y \hat{\mathbf{s}}) \cdot \nabla g^* \\ & - g^* (i y_c \hat{\mathbf{n}} + y \hat{\mathbf{s}}) \cdot \nabla f] \, ds. \end{aligned} \tag{3.2}$$

If we make

$$S = S(\mathbf{r}) = \delta(\mathbf{r} - \mathbf{r}') \tag{3.3}$$

in (2.7), where δ denotes the Dirac delta function, we may define a unique Green's function $G(y_c; \mathbf{r}; \mathbf{r}')$ for the operator $\mathscr{L}(y_c)$, satisfying

$$\mathscr{L}(y_c) G(y_c; \mathbf{r}; \mathbf{r}') = \delta(\mathbf{r} - \mathbf{r}') \tag{3.4}$$

and the boundary condition

$$G(y_c; \mathbf{r}; \mathbf{r}') \to 0, \qquad |\mathbf{r}| \to \infty. \tag{3.5}$$

In our notation for G, we adopt the convention that the first position vector denotes an observation point, while the second gives the position of the source.

Most Green's functions encountered in the literature refer to self-adjoint boundary value problems, giving rise to simple symmetry properties with respect to the exchange of the position arguments. However, (3.2) indicates that the present problem is not self-adjoint (Friedman, 1956). A symmetry relation for $G(y_c; \mathbf{r}; \mathbf{r}')$ may be obtained by choosing

$$f(\mathbf{r}) = G(y_c; \mathbf{r}; \mathbf{r}_1), \qquad g(\mathbf{r}) = G(y_c^*; \mathbf{r}; \mathbf{r}_2) \tag{3.6}$$

in the identity (3.2), and extending the region B to infinity. The boundary integral in (3.2) will then vanish provided that the Green's function decays fast enough as

$|\mathbf{r}| \to \infty$. From the results given in Section 4, it will be clear that G decays exponentially as $|\mathbf{r}| \to \infty$, provided $A \neq 0$. Using (3.6) in (3.2), one easily gets, in view of (3.4), the desired symmetry relation

$$G(y_c; \mathbf{r}_1; \mathbf{r}_2) = -[G(y_c^*; \mathbf{r}_2; \mathbf{r}_1)]^*. \tag{3.7}$$

The identity (3.2) may be used to derive an integral representation for the pressure perturbation field. Choosing $f = p(\mathbf{r}, \omega)$, and leaving g arbitrary for the moment, it is seen from (2.7) that the first term on the left in (3.2) becomes $\langle S, g \rangle$, which depends only on the forcing field $\mathbf{F}'$. Using (2.13), the second term in the integrand in (3.2) can be written in terms of $\mathbf{F}'$ and q. The remaining terms in Green's identity will depend on p, but not on the derivatives of p. A particularly interesting form for the second term on the left in (3.2) emerges when we choose the arbitrary function g as

$$g(\mathbf{r}) = -G(y_c^*; \mathbf{r}; \mathbf{r}'). \tag{3.8}$$

We have

$$\langle p, \mathscr{L}(y_c^*)g \rangle = -\langle p, \mathscr{L}(y_c^*)G(y_c^*; \mathbf{r}; \mathbf{r}') \rangle = -\langle p, \delta(\mathbf{r} - \mathbf{r}') \rangle = -p(\mathbf{r}'), \tag{3.9}$$

provided $\mathbf{r}'$ lies inside B (note that the result of the above calculation is zero if $\mathbf{r}'$ lies outside B). Using the symmetry relation (3.7), one obtains after some algebra the following integral representation for the pressure perturbation at interior points $\mathbf{r}'$ in terms of the pressure distribution at the boundary:

$$\begin{aligned} p(\mathbf{r}') = {} & \oint_\Gamma p(\mathbf{r})\hat{\mathbf{n}}(s) \cdot \mathbf{K}(y_c; \mathbf{r}'; \mathbf{r})\, ds - \tfrac{1}{2}\rho_o c \oint_\Gamma q(s) G(y_c; \mathbf{r}'; \mathbf{r})\, ds \\ & - \iint_B \mathbf{F}'(\mathbf{r}) \cdot \mathbf{K}(y_c; \mathbf{r}'; \mathbf{r})\, dx\, dy, \end{aligned} \tag{3.10}$$

where the vector $\mathbf{K}$ is defined as

$$\mathbf{K}(y_c; \mathbf{r}'; \mathbf{r}) = -(y^2 - y_c^2)^{-1}(iy_c + y\hat{\mathbf{z}} \times)\nabla G(y_c; \mathbf{r}'; \mathbf{r}). \tag{3.11}$$

Note that the vector $\mathbf{r}$ which appears in the boundary integrals in (3.10) varies along the boundary, $\mathbf{r} = \mathbf{r}(s)$. Note also that the gradient operator in (3.11) acts on the second position argument, instead of on the first, as in (3.4).

The integral representation (3.10) is an alternative formulation of our boundary value problem for the shallow water equations. Physically, (3.10) states that the pressure perturbation at an arbitrary point $\mathbf{r}'$ inside B is determined by the following factors: (a) the pressure perturbations along the boundary, (b) the normal outflow distribution, and (c) the forcing distribution over the considered region. The influence of each of these factors acting at any point $\mathbf{r}$ is "propagated" to the point $\mathbf{r}'$ through the kernel functions $G(y_c; \mathbf{r}'; \mathbf{r})$ and $\mathbf{K}(y_c; \mathbf{r}'; \mathbf{r})$. Therefore, if we know the pressure distribution along the boundary, the pressure perturbation at any interior point $\mathbf{r}'$ can be directly computed from (3.10), provided we are able to evaluate the

kernel functions appearing in this equation. In Section 4, we present a rather complete discussion on the computation of the kernel functions. The boundary pressure distribution is obtained by solving the basic BIE of the theory, which is derived in Section 5 by allowing the interior point $\mathbf{r}'$ in (3.10) to approach the boundary.

Knowing the pressure values along the boundary, one can also compute the interior velocity field. Substituting the value of p given by (3.10) in (2.5), one gets an expression for the velocity,

$$\begin{aligned}\mathbf{u}(\mathbf{r}') = (2/\rho_o c)\Big[&(y'^2 - y_c^2)^{-1}(iy_c - y'\hat{\mathbf{z}}\times)\mathbf{F}'(\mathbf{r}') \\ &+ \iint_B \mathscr{D}(y_c;\mathbf{r}';\mathbf{r})\cdot\mathbf{F}'(\mathbf{r})\,dx\,dy \\ &- \oint_\Gamma p(\mathbf{r})\mathscr{D}(y_c;\mathbf{r}';\mathbf{r})\cdot\hat{\mathbf{n}}(s)\,ds\Big] \\ &- \oint_\Gamma q(s)\mathbf{J}(y_c;\mathbf{r}';\mathbf{r})\,ds,\end{aligned} \tag{3.12}$$

where the vector $\mathbf{J}$ and the tensor $\mathscr{D}$ are given by

$$\mathbf{J}(y_c;\mathbf{r}';\mathbf{r}) = -(y'^2 - y_c^2)^{-1}(iy_c - y'\hat{\mathbf{z}}\times)\nabla' G(y_c;\mathbf{r}';\mathbf{r}), \tag{3.13}$$

$$\mathscr{D}(y_c;\mathbf{r}';\mathbf{r}) = (y'^2 - y_c^2)^{-1}(iy_c - y'\hat{\mathbf{z}}\times)\nabla'\mathbf{K}(y_c;\mathbf{r}';\mathbf{r}). \tag{3.14}$$

The Green's function G, the vectors $\mathbf{K}$ and $\mathbf{J}$, and the tensor $\mathscr{D}$ are the basic influence functions of the equatorial β-plane shallow water equations. As shown in (3.10) and (3.12), the use of these functions constitutes a systematic way of representing solutions to these equations.

4. Kernels

In this section, the Green's function and the kernel functions appearing in the integral relations (3.10) and (3.12) are expanded in series of meridional modes (Hermite functions). In order to overcome some troubles with the convergence of the series, we apply a new asymptotic technique of summation of Hermite series (Holvorcem, 1992). This technique allows not only a more efficient evaluation of the series, but also gives information about the behavior of the kernel functions when the observation point is close to the source. Such information is crucial in any practical implementation of (3.10) as a numerical tool.

a. Analytic expressions. The partial differential equation (3.4) defining the Green's function has coefficients which depend only on y. Therefore, we may treat this equation by taking a Fourier transform in the zonal direction,

$$f(\alpha) = \int_{-\infty}^{\infty} e^{i\alpha x} f(x)\,dx. \tag{4.1}$$

The transformed version of (3.4) is the ordinary differential equation

$$\frac{d}{dy}\left[(y^2 - y_c^2)^{-1}\frac{d}{dy}G(\alpha, y; \mathbf{r}')\right] - \left[\frac{1}{4} + \alpha(\alpha + y_c^{-1})(y^2 - y_c^2)^{-1} + 2\alpha y_c(y^2 - y_c^2)^{-2}\right] G(\alpha, y; \mathbf{r}') = iy_c^{-1}e^{i\alpha x'}\delta(y - y'). \tag{4.2}$$

(For brevity, in the rest of this paper we shall consistently write the Green's function G and the kernels $\mathbf{K}$, $\mathbf{J}$ and $\mathscr{D}$ without the argument y_c.) To construct the solution of (4.2) which is compatible with the boundary conditions (3.5), we need a solution $h(y)$ of the associated homogeneous equation, which vanishes as $y \to \infty$ (Butkov, 1968). By the symmetry of (4.2), $h(-y)$ will be a second solution vanishing as $y \to -\infty$. It can be verified that a solution of the homogeneous equation with the desired behavior as $y \to \infty$ is

$$h(y) = \alpha(y/y_c)U(a, y) - U'(a, y), \tag{4.3}$$

where $U(a, y)$ denotes a parabolic cylinder function (Abramowitz and Stegun, 1965), $U'(a, y) = \partial U(a, y)/\partial y$ and

$$a = \alpha(\alpha + y_c^{-1}) - y_c^2/4. \tag{4.4}$$

The solution to the inhomogeneous equation (4.2) is then (Vianna, 1988)

$$G(\alpha, y; \mathbf{r}') = -iy_c^{-1}e^{i\alpha x'}(y'^2 - y_c^2)\frac{h(-\epsilon y')h(\epsilon y)}{W(y')}, \tag{4.5}$$

where

$$\epsilon = \text{sign}\,(y - y') \tag{4.6}$$

and $W(y')$ denotes the Wronskian of $h(y')$ and $h(-y')$. Using standard properties of $U(a, y)$, we can show that

$$W(y') = (2\pi)^{1/2}\frac{[1 - (2\alpha/y_c)^2]}{4\Gamma(a + 1/2)}(y'^2 - y_c^2). \tag{4.7}$$

In (4.5), the numerator and the denominator present a common factor $(1 + 2\alpha/y_c)^2$, which corresponds to the spurious root $\alpha = -y_c/2$ of the dispersion relations of the equatorial β-plane (Matsuno, 1966). In order to cancel out this factor, it is convenient to express $h(y)$ in terms of parabolic cylinder functions of order $a + 1$, and to express $\Gamma(a + \frac{1}{2})$ in (4.7) in terms of $\Gamma(a + \frac{3}{2})$. With these transformations, (4.5) becomes

$$G(\alpha, y; \mathbf{r}') = (2\pi)^{-1/2}\frac{i\Gamma(a + 3/2)e^{i\alpha x'}\tilde{h}(\epsilon y)\tilde{h}(-\epsilon y')}{(\alpha - y_c/2)[1 + y_c(\alpha - y_c/2)]}, \tag{4.8}$$

where

$$\tilde{h}(y) = [y^2/2 + y_c(\alpha - y_c/2) + 1]U(a+1, y) - yU'(a+1, y). \tag{4.9}$$

The Green's function is given by the inverse Fourier transform

$$G(\mathbf{r}; \mathbf{r}') = (2\pi)^{-1} \int_{-\infty}^{\infty} e^{-i\alpha x} G(\alpha, y; \mathbf{r}')\, d\alpha. \tag{4.10}$$

To evaluate (4.10) by residue integration, we must study the singularities of $G(\alpha, y; \mathbf{r}')$ in the complex α-plane. In (4.8), $\tilde{h}(\epsilon y)$ and $\tilde{h}(-\epsilon y')$ are analytic functions of α. The function $\Gamma(z)$ has simple poles at $z = -m$, $m = 0, 1, 2, \ldots$, with residue $(-1)^m/m!$. Therefore, (4.8) will have poles when $a + \frac{1}{2} = -m$, i.e.,

$$\alpha = -\gamma \pm \lambda_m, \qquad m = 0, 1, 2, \ldots \tag{4.11}$$

where

$$\begin{aligned} \gamma &= (2y_c)^{-1}, & \lambda_m &= i(\tilde{m} - Q)^{1/2}, \\ \tilde{m} &= m + \tfrac{1}{2}, & Q &= (y_c^2 + y_c^{-2})/4. \end{aligned} \tag{4.12}$$

The remaining poles of (4.8) are clearly

$$\alpha = \alpha_{-1} = y_c/2 - y_c^{-1}, \qquad \alpha = \alpha_{-2} = y_c/2, \tag{4.13}$$

which correspond to (4.11) with the plus sign and $m = -1, -2$. These poles represent the Yanai and Kelvin modes, respectively. When the dissipation is small ($\Delta\omega \ll \omega$), the poles (4.13) lie in the lower half of the α-plane, close to the real axis, thus representing propagating waves. The poles with the plus (minus) sign in (4.11) lie in the upper (lower) half plane. If $\Delta\omega \ll \omega$, the poles (4.11) with $m = 0, 1, \ldots, M_Q = [\![\mathrm{Re}\, Q - \tfrac{1}{2}]\!]$ (the brackets $[\![\ ]\!]$ denote the integer part) lie close to the real axis, corresponding to the propagating Rossby (inertia-gravity) modes when the frequency is low (high) enough. In this case, the poles with $m \geq M_Q$ are strongly damped in the zonal direction.

To evaluate the integral (4.10), one must sum up the residues at the poles in the upper (lower) half plane when $x - x'$ is negative (positive), in order to ensure that the integrand decays as $|\alpha| \to \infty$ in that half plane. Using the recurrence relations of the parabolic cylinder functions, one can show that

$$\begin{aligned} G(\mathbf{r}; \mathbf{r}') = {} & 2^{-3/2}(1-\sigma)\{\exp[-i\alpha_{-2}(x-x')]\psi_o(y/\sqrt{2})\psi_o(y'/\sqrt{2}) \\ & + \exp[-i\alpha_{-1}(x-x')]\psi_1(y/\sqrt{2})\psi_1(y'/\sqrt{2})\} \\ & - 2^{-1/2}\gamma \sum_{m=0}^{\infty} \frac{\exp[-i(\sigma\lambda_m - \gamma)(x-x')]}{\lambda_m(\sigma\lambda_m - \lambda_{-1})(\sigma\lambda_m - \lambda_{-2})} \phi_m^{\sigma}(y)\phi_m^{\sigma}(y'), \end{aligned} \tag{4.14}$$

where

$$\sigma = \mathrm{sign}(x' - x), \qquad \lambda_{-1} = \alpha_{-1} + \gamma, \qquad \lambda_{-2} = \alpha_{-2} + \gamma, \tag{4.15}$$

$$\phi_m^\sigma(y) = (m+1)^{1/2} y\psi_{m+1}(y/\sqrt{2}) + \alpha_{-2}(\sigma\lambda_m - \lambda_{-1})\,(m+1)^{-1/2}[y\psi_{m+1}(y/\sqrt{2}) + 2^{1/2}\psi'_{m+1}(y/\sqrt{2})], \tag{4.16}$$

and

$$\psi_m(z) = (m!\sqrt{\pi})^{-1/2} U(-(m+\tfrac{1}{2}), \sqrt{2}z) = (2^m m!\sqrt{\pi})^{-1/2} e^{-z^2/2} H_m(z) \tag{4.17}$$

is the Hermite function of order m.

The physical interpretation of (4.14) for small dissipation ($\Delta\omega \ll \omega$) is the following: when the observation point $\mathbf{r}$ lies to the east of the source at $\mathbf{r}'$, the first two terms represent the Kelvin and Rossby-gravity waves which are emitted by the source towards $\mathbf{r}$. The terms with $m = 0, 1, \ldots, M_Q - 1$ represent short Rossby waves or inertia-gravity waves with eastward group velocity, depending on the frequency. When $\mathbf{r}$ lies to the west of $\mathbf{r}'$, the first two terms of (4.14) are obviously absent; the terms with $m = 0, 1, \ldots, M_Q - 1$ represent long Rossby waves or inertia-gravity waves with westward group velocity, depending on the frequency. The terms with $m \geq M_Q$ represent a set of damped modes, which remain trapped near the source's meridian $x = x'$.

From (4.11), (4.12) and (4.14), we see that the damped mode of index m decays to e^{-1} of its amplitude at $x = x'$ at a non-dimensional distance $[\mathrm{Re}(\tilde{m} - Q)^{1/2}]^{-1}$ from the meridian. This observation is important for the numerical evaluation of (4.14). In fact, for small dissipation it is sufficient to truncate the series at

$$m \approx \mathrm{Re}\, Q + [b/(x - x')]^2, \tag{4.18}$$

with b a positive constant, to ensure that the last term retained has at longitude x only e^{-b} of its amplitude at $x = x'$, and that the higher order modes are even more strongly damped. However, (4.18) indicates that as $x \to x'$ it will be necessary to retain an infinite number of terms in (4.14). Accordingly, in trying to evaluate (4.14) by direct summation, one verifies that the series converges very slowly when $|x - x'|$ is less than one or two deformation radii. The asymptotic methods described later in this section will present an effective solution to this difficulty.

Using (4.14) in the definitions (3.11), (3.13) and (3.14), it is possible to express the kernels $\mathbf{K}$, $\mathbf{J}$ and $\mathscr{D}$ as series of Hermite functions. Using the recurrence relations of parabolic cylinder functions, one can show that

$$(y^2 - y_c^2)^{-1}(iy_c \pm y\hat{\mathbf{z}} \times)\nabla\{\exp[\pm i(\sigma\lambda_m - \gamma)x]\phi_m^\sigma(y)\} = \pm \exp[\pm i(\sigma\lambda_m - \gamma)x]\,[\zeta_m^\sigma(y)\hat{\mathbf{x}} \pm i\theta_m^\sigma(y)\hat{\mathbf{y}}], \tag{4.19}$$

where

$$\zeta_m^\sigma(y) = -2^{-1/2}(m+1)^{1/2}\psi'_{m+1}(y/\sqrt{2}) - 2^{-1}\alpha_{-2}(\sigma\lambda_m - \lambda_{-1})\,(m+1)^{-1/2}[2^{1/2}\psi'_{m+1}(y/\sqrt{2}) + y\psi_{m+1}(y/\sqrt{2})], \tag{4.20}$$

$$\theta_m^\sigma(y) = (\sigma\lambda_m - \lambda_{-2})\,(m+1)^{1/2}\psi_{m+1}(y/\sqrt{2}). \tag{4.21}$$

The identity (4.19) implies that the factors $(y^2 - y_c^2)^{-1}$, $(y'^2 - y_c^2)^{-1}$ which appear in the definitions of **K**, **J** and $\mathscr{D}$ do not introduce any singular behavior at $y = \pm y_c$. The expansions for **K**, **J** and $\mathscr{D}$ in series of Hermite functions are:

$$\begin{aligned}\mathbf{K}(\mathbf{r};\mathbf{r}') = {} & 2^{-5/2}(\sigma - 1)\{\exp[-i\alpha_{-2}(x - x')]\psi_o(y/\sqrt{2})\psi_o(y'/\sqrt{2})\hat{\mathbf{x}} \\ & + \exp[-i\alpha_{-1}(x - x')]\psi_1(y/\sqrt{2})[\psi_1(y'/\sqrt{2})\hat{\mathbf{x}} - 4i\gamma\psi_o(y'/\sqrt{2})\hat{\mathbf{y}}]\} \\ & + 2^{-1/2}\gamma\sum_{m=0}^{\infty}\frac{\exp[-i(\sigma\lambda_m - \gamma)(x - x')]}{\lambda_m(\sigma\lambda_m - \lambda_{-1})(\sigma\lambda_m - \lambda_{-2})}\phi_m^{\sigma}(y)[\zeta_m^{\sigma}(y')\hat{\mathbf{x}} + i\theta_m^{\sigma}(y')\hat{\mathbf{y}}],\end{aligned} \tag{4.22}$$

$$\begin{aligned}\mathbf{J}(\mathbf{r};\mathbf{r}') = {} & 2^{-5/2}(1 - \sigma)\{\exp[-i\alpha_{-2}(x - x')]\psi_o(y'/\sqrt{2})\psi_o(y/\sqrt{2})\hat{\mathbf{x}} \\ & + \exp[-i\alpha_{-1}(x - x')]\psi_1(y'/\sqrt{2})[\psi_1(y/\sqrt{2})\hat{\mathbf{x}} + 4i\gamma\psi_o(y/\sqrt{2})\hat{\mathbf{y}}]\} \\ & - 2^{-1/2}\gamma\sum_{m=0}^{\infty}\frac{\exp[-i(\sigma\lambda_m - \gamma)(x - x')]}{\lambda_m(\sigma\lambda_m - \lambda_{-1})(\sigma\lambda_m - \lambda_{-2})}\phi_m^{\sigma}(y')[\zeta_m^{\sigma}(y)\hat{\mathbf{x}} - i\theta_m^{\sigma}(y)\hat{\mathbf{y}}],\end{aligned} \tag{4.23}$$

$$\begin{aligned}\mathscr{D}(\mathbf{r};\mathbf{r}') = {} & 2^{-7/2}(1 - \sigma)\{\exp[-i\alpha_{-2}(x - x')]\psi_o(y/\sqrt{2})\psi_o(y'/\sqrt{2})\hat{\mathbf{x}}\hat{\mathbf{x}} \\ & + \exp[-i\alpha_{-1}(x - x')][\psi_1(y/\sqrt{2})\hat{\mathbf{x}} + 4i\gamma\psi_o(y/\sqrt{2})\hat{\mathbf{y}}][\psi_1(y'/\sqrt{2})\hat{\mathbf{x}} \\ & - 4i\gamma\psi_o(y'/\sqrt{2})\hat{\mathbf{y}}]\} - 2^{-1/2}\gamma\sum_{m=0}^{\infty}\frac{\exp[-i(\sigma\lambda_m - \gamma)(x - x')]}{\lambda_m(\sigma\lambda_m - \lambda_{-1})(\sigma\lambda_m - \lambda_{-2})} \\ & \cdot[\zeta_m^{\sigma}(y)\hat{\mathbf{x}} - i\theta_m^{\sigma}(y)\hat{\mathbf{y}}][\zeta_m^{\sigma}(y')\hat{\mathbf{x}} + i\theta_m^{\sigma}(y')\hat{\mathbf{y}}]\end{aligned} \tag{4.24}$$

(The juxtaposition of two vectors, as in (4.24), denotes the dyad or tensor product.)

b. Asymptotic summation techniques. To understand the contribution of the damped equatorial modes to the Green's function (4.14) and the kernels (4.22)–(4.24), it is convenient to study the asymptotic behavior of the general terms in their Hermite expansions as $m \to \infty$. Asymptotic expansions for Hermite functions of large order, valid if $m \gg 1, y^2/4$, are (Holvorcem, 1992)

$$\begin{aligned}\psi_{m+1}(y/\sqrt{2}) \sim {} & i(8\pi^2\tilde{m})^{-1/4}\sum_{\epsilon=\pm 1}\epsilon i^{\epsilon m}\exp[-i\epsilon\chi(\tilde{m},y)] \\ & \cdot[1 + (y^2/16)\tilde{m}^{-1} - i\epsilon(y/16)\tilde{m}^{-3/2} + \cdots]\end{aligned} \tag{4.25}$$

$$\begin{aligned}\psi'_{m+1}(y/\sqrt{2}) \sim {} & (\tilde{m}/2\pi^2)^{1/4}\sum_{\epsilon=\pm 1} i^{\epsilon m}\exp[-i\epsilon\chi(\tilde{m},y)] \\ & \cdot[1 - (y^2/16)\tilde{m}^{-1} + i\epsilon(y/16)\tilde{m}^{-3/2} + \cdots]\end{aligned} \tag{4.26}$$

where $\tilde{m} = m + \frac{1}{2}$ and

$$\chi(\tilde{m},y) = \tilde{m}[\sin^{-1}\tau + \tau(1 - \tau^2)^{1/2}], \qquad \tau = \tau(\tilde{m},y) = y/2\tilde{m}^{1/2}. \tag{4.27}$$

In view of (4.12), (4.13) and (4.15), the coefficients of ψ_{m+1} and ψ'_{m+1} in the expressions for ϕ_m^{σ}, ζ_m^{σ} and θ_m^{σ} (Eqs. (4.16), (4.20) and (4.21)) can be expanded in powers of $\tilde{m}^{-1/2}$ provided $m \gg 1, |Q|$. Using (4.25) and (4.26), one then obtains after some algebra the following asymptotic expansions for ϕ_m^{σ}, ζ_m^{σ} and θ_m^{σ}, valid if $m \gg 1$,

$|Q|, y^2/4$:

$$\phi_m^\sigma(y) \sim (\tilde{m}/8\pi^2)^{1/4} \sum_{\epsilon=\pm 1} i^{\epsilon m} \exp\left[-i\epsilon\chi(\tilde{m}, y)\right] \sum_{k=0}^{\infty} (i\sigma)^{k+1} A_k(\sigma\epsilon y)\tilde{m}^{-k/2}, \tag{4.28}$$

$$\zeta_m^\sigma(y) \sim -(\tilde{m}^3/8\pi^2)^{1/4} \sum_{\epsilon=\pm 1} i^{\epsilon m} \exp\left[-i\epsilon\chi(\tilde{m}, y)\right] \sum_{k=0}^{\infty} (i\sigma)^k B_k(\sigma\epsilon y)\tilde{m}^{-k/2}, \tag{4.29}$$

$$\theta_m^\sigma(y) \sim -\sigma(\tilde{m}^3/8\pi^2)^{1/4} \sum_{\epsilon=\pm 1} \epsilon i^{\epsilon m} \exp\left[-i\epsilon\chi(\tilde{m}, y)\right] \sum_{k=0}^{\infty} (i\sigma)^k C_k(\sigma\epsilon y)\tilde{m}^{-k/2}, \tag{4.30}$$

where the first $A_k(y), B_k(y), C_k(y)$ are given by

$$\begin{aligned} &A_0(y) = y + y_c, \qquad A_1(y) = (\tfrac{1}{2})\,(y_c^2 - 1 + y_c y), \\ &A_2(y) = (\tfrac{1}{16})\,[y_c(y^2 + 8Q - 4) + y(4y_c^2 - y^2)], \\ &A_3(y) = (\tfrac{1}{32})\,[4(1 - y_c^2) + (y_c^2 + 1)y^2 + y_c y(8Q - 6 - y^2)], \end{aligned} \tag{4.31}$$

$$\begin{aligned} &B_0(y) = 1, \qquad B_1(y) = \alpha_{-2}, \qquad B_2(y) = (\tfrac{1}{16})\,(4y_c^2 + y^2 + 4y_c y), \\ &B_3(y) = (\tfrac{1}{32})\,[y_c(8Q + y^2 - 4) + 2y(2y_c^2 - 3)], \end{aligned} \tag{4.32}$$

$$\begin{aligned} &C_0(y) = 1, \qquad C_1(y) = \lambda_{-2}, \qquad C_2(y) = (\tfrac{1}{16})\,(8Q + 4 - y^2), \\ &C_3(y) = (\tfrac{1}{16})\,[y - \lambda_{-2}(y^2 - 4)]. \end{aligned} \tag{4.33}$$

To determine the asymptotic behavior of the terms of (4.14) and (4.22)–(4.24), we need also the expansion

$$[\lambda_m(\sigma\lambda_m - \lambda_{-1})\,(\sigma\lambda_m - \lambda_{-2})]^{-1} \sim i\tilde{m}^{-3/2} \sum_{k=0}^{\infty} (i\sigma)^k \eta_k \tilde{m}^{-k/2}, \tag{4.34}$$

where the first η_k are given by

$$\eta_0 = 1, \qquad \eta_1 = -y_c, \qquad \eta_2 = \alpha_{-2}^2 + \lambda_{-1}\lambda_{-2}/2, \qquad \eta_3 = 0. \tag{4.35}$$

By (4.12), (4.13) and (4.15), this expansion holds for $m \gg 1, |Q|$.

From (4.28) and (4.34), one easily shows that the asymptotic behavior of the general term g_m in the series (4.14) is given by

$$\begin{aligned} g_m \sim i(\gamma/4\pi) \exp\left[-i(\sigma\lambda_m - \gamma)\,(x - x')\right] \sum_{\mu,\epsilon=\pm 1} i^{(\epsilon+\mu)m} \exp\big\{-i[\epsilon\chi(\tilde{m}, y) \\ + \mu\chi(\tilde{m}, y')]\big\} \sum_{k=0}^{\infty} (i\sigma)^k G_k(\sigma\epsilon y, \sigma\mu y')\tilde{m}^{-k/2-1}, \end{aligned} \tag{4.36}$$

where

$$G_k(y, y') = \sum_{n=0}^{k} \eta_{k-n} \sum_{j=0}^{n} A_j(y) A_{n-j}(y'), \tag{4.37}$$

provided $m \gg 1$, $|Q|$, $y^2/4$, $y'^2/4$. These expressions show clearly why (4.14) converges so slowly near the source's meridian: if $x = x'$, then $|g_m| = O(m^{-1})$ as $m \to \infty$, so that the series is conditionally convergent (Holvorcem, 1992). Now, if

$$M \gg 1, |Q|, y^2/4, y'^2/4 \tag{4.38}$$

then (4.36) implies that the Green's function (4.14) is given asymptotically by

$$G(\mathbf{r}; \mathbf{r}') \sim \sum_{m=-2}^{M-1} g_m + i(\gamma/4\pi) \exp[i\gamma(x - x')] \sum_{k=0}^{\infty} (i\sigma)^k \cdot \sum_{\mu,\epsilon=\pm 1} S_{k+2}\left(\frac{\mu + \epsilon}{2}; x, x'; \epsilon y, \mu y'\right) G_k(\sigma\epsilon y, \sigma\mu y'), \tag{4.39}$$

where g_{-1} and g_{-2} denote the terms of (4.14) corresponding to the Yanai and Kelvin waves, respectively, and

$$S_k(\nu; x, x'; y, y') = \sum_{m=\tilde{M}}^{\infty} (-1)^{m} \tilde{m}^{-k/2} \exp[-\Phi(\tilde{m}; x, x'; y, y')], \tag{4.40}$$

$$\Phi(\tilde{m}; x, x'; y, y') = (\tilde{m} - Q)^{1/2}|x - x'| + i[\chi(\tilde{m}, y) + \chi(\tilde{m}, y')]. \tag{4.41}$$

Using (4.38)–(4.40) and the expressions for the coefficients A_k, η_k and G_k, it can be shown that the expansion (4.39) converges rapidly with k. However, if $x \to x'$ and k is small the series $S_k(\nu; x; x'; y, y')$ converges very slowly with m, so that it is uneconomical to evaluate it by summing (4.40) directly. Fortunately, the series may be summed asymptotically (Holvorcem, 1992) as

$$S_k(\pm 1; x, x'; y, y') \sim 2^{-1}(-1)^{M} \tilde{M}^{-k/2} \exp[-\Phi(\tilde{M}; x, x'; y, y')]\{1 + \tfrac{1}{4}\xi_0 \tilde{M}^{-1/2} + \tfrac{1}{4}k\tilde{M}^{-1} - \tfrac{1}{4}(\xi_0^3/48 + \xi_1)\tilde{M}^{-3/2} - \tfrac{1}{64}(k-1)\xi_0^2\tilde{M}^{-2} + \cdots\}, \tag{4.42}$$

$$S_k(0; x, x'; y, y') \sim I_k(x, x'; y, y') + 2^{-1}\tilde{M}^{-k/2} \exp[-\Phi(\tilde{M}; x, x'; y, y')]\{1 + \tfrac{1}{12}\xi_0 \tilde{M}^{-1/2} + \tfrac{1}{12}k\tilde{M}^{-1} - \tfrac{1}{12}(\xi_0^3/240 + \xi_1)\tilde{M}^{-3/2} - \tfrac{1}{960}(k+1)\xi_0^2\tilde{M}^{-2} + \cdots\}, \tag{4.43}$$

where $\tilde{M} = M + \tfrac{3}{2}$. Here the coefficients $\xi_n = \xi_n(x, x'; y, y')$ are defined by the expansion

$$\Phi(\tilde{m}; x, x'; y, y') = \tilde{m}^{1/2}(\xi_0 + \xi_1\tilde{m}^{-1} + \xi_2\tilde{m}^{-2} + \cdots); \tag{4.44}$$

the first ξ_n are given explicitly by

$$\begin{aligned} \xi_0(x, x'; y, y') &= |x - x'| + i(y + y'), \\ \xi_1(x, x'; y, y') &= -(Q/2)|x - x'| + (y^3 + y'^3)/24i. \end{aligned} \tag{4.45}$$

The function I_k which appears in (4.43) is defined by

$$I_k(x, x'; y, y') = \int_{\tilde{M}}^{\infty} \tilde{m}^{-k/2} \exp[-\Phi(\tilde{m}; x, x'; y, y')]\, d\tilde{m}, \tag{4.46}$$

Table 1. Computation of $G(y_c;\ \mathbf{r};\ \mathbf{r}')$ for $y_c = 0.2639 - 0.002\,i, y = 3, y' = 2$ and $x - x' = 10^{-5}$. The second column shows the value of (4.14) truncated at $m = M - 1$, and the third column is computed from (4.39) (truncated at $k = 3$), (4.42) and (4.43).

M	Partial sum	Asymptotic value
11	6.3477 + 1.9305i	6.3770 + 2.1681i
15	6.3311 + 2.5979i	6.3765 + 2.1954i
19	6.3582 + 2.7969i	6.3765 + 2.2005i
26	6.3864 + 2.8644i	6.3766 + 2.2021i

and may be evaluated either asymptotically or by a convergent series expansion (see the Appendix for details). It follows from (4.38) that the expansions (4.42) and (4.43) are rapidly convergent; the displayed terms are sufficient to obtain the sum of $S_k(\nu; x, x'; y, y')$ accurate to a few percent (Holvorcem, 1992).

For computational purposes, it is important to know the maximum values of M which may occur in the application of (4.39) to the real oceans. As an example, consider the second baroclinic mode of the tropical Atlantic Ocean, for which du Penhoat and Treguier (1985) give the vertical eigenvalue $c = 1.26$ m s $^{-1}$. The corresponding radius of deformation is $R_o = 167$ km, and by (2.11) we have for small friction $y_c \simeq \mathrm{Re}\, y_c = \omega/\omega_o$, where $\omega_o = \beta R_o = 3.81 \times 10^{-6} \mathrm{s}^{-1}$. The maximum values of $|Q|$ occur at very low or very high frequencies; at the annual frequency, $y_c \simeq 0.05$, implying that $|Q| \simeq 90$. Considering, as usual, an ocean model extending from 20S to 20N, the maximum value of y or y' is nearly 13, so that $y^2/4, y'^2/4 \lesssim 42$. Now, to compute $S_k(\nu; x, x'; y, y')$ with an error of a few percent, we may take M as 3 times the largest term in the right-hand side of (4.38) (Holvorcem, 1992), so that M is not expected to exceed a few hundreds in real applications.

In Table 1, we give an example of the numerical use of (4.39) when $|x - x'|$ is very small (10^{-5} in non-dimensional units), so that we expect (4.14) to converge very slowly. We note that the value of $G(\mathbf{r}; \mathbf{r}')$ computed from (4.39) is accurately constant irrespective of the chosen value of M, while the partial sum of (4.14) truncated at $m = M - 1$ does not yield a definite result. From numerical experiments with the expansion (4.39), we have concluded that it may in practice be truncated at $k = 3$.

In Figure 1, we show a contour map of Im $G(\mathbf{r}; \mathbf{r}')$ for a source at $\mathrm{r}' = (0, 1)$ and for three different frequencies (friction is negligible). The values of G were computed using the truncation (4.18) with $b = 7$ whenever $|x| > 0.5$, and using (4.39) for $|x| < 0.5$. Note in the figures that the field is continuous across the meridian $x = 0$, a property which is not apparent from the series representation (4.14). In Figure 1a, the frequency is low, with Rossby waves appearing to the east and west of the source; Figure 1c shows a high-frequency case, dominated by inertia-gravity waves; finally, Figure 1b shows an "intermediate" frequency case, where the only propagating modes are the Kelvin and Yanai waves.

In Figure 2, we illustrate how the Green's function field depends on the position of

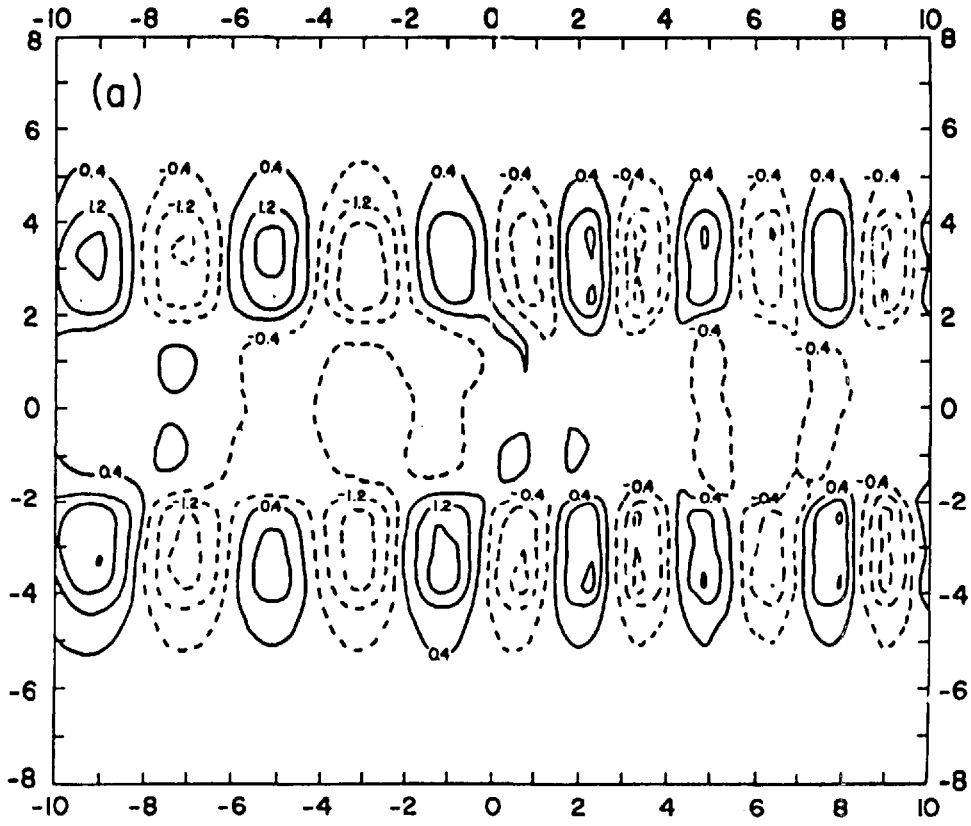

Figure 1. Imaginary part of the almost dissipation-free Green's function $G(y_c; \mathbf{r}; \mathbf{r}')$, with the source at $\mathbf{r}' = (0, 1)$, for three non-dimensional frequencies: (a) $y_c = 0.263$, (b) $y_c = 0.789$, (c) $y_c = 3.16$. The units in both axes are non-dimensionalized by the equatorial deformation radius $R_o = (c/2\beta)^{1/2}$. The logarithmic singularity of G at $\mathbf{r} = \mathbf{r}'$ (see Section 4c) is not apparent in these figures.

the source, at a fixed frequency. It is known (Jacobs, 1967; Ripa, 1989) that the radiation of a point source of frequency ω on the β-plane will form a system of multiple caustics, whose envelope consists of the "extreme latitudes" $y = \pm 2\,|Q|^{1/2}$. These latitudes are indicated by dashed lines in Figure 2. When the source lies within the extreme latitudes (Fig. 2a), the field of G is also confined there. If the source is placed outside the extreme latitudes (Fig. 2c), the amplitude of G is negligible everywhere, except in the immediate neighborhood of the source. An intermediate case, where the source is placed on an extreme latitude, is shown in Figure 2b.

The maps in Figures 1 and 2 suggest that G always decays exponentially when $|y| \to \infty$, and this conclusion is supported by ray theory (Jacobs, 1967; Ripa, 1989). When $|x| \to \infty$, only a finite number of propagating modes contribute to the Green's function, and these will decay exponentially in the direction of their group velocities,

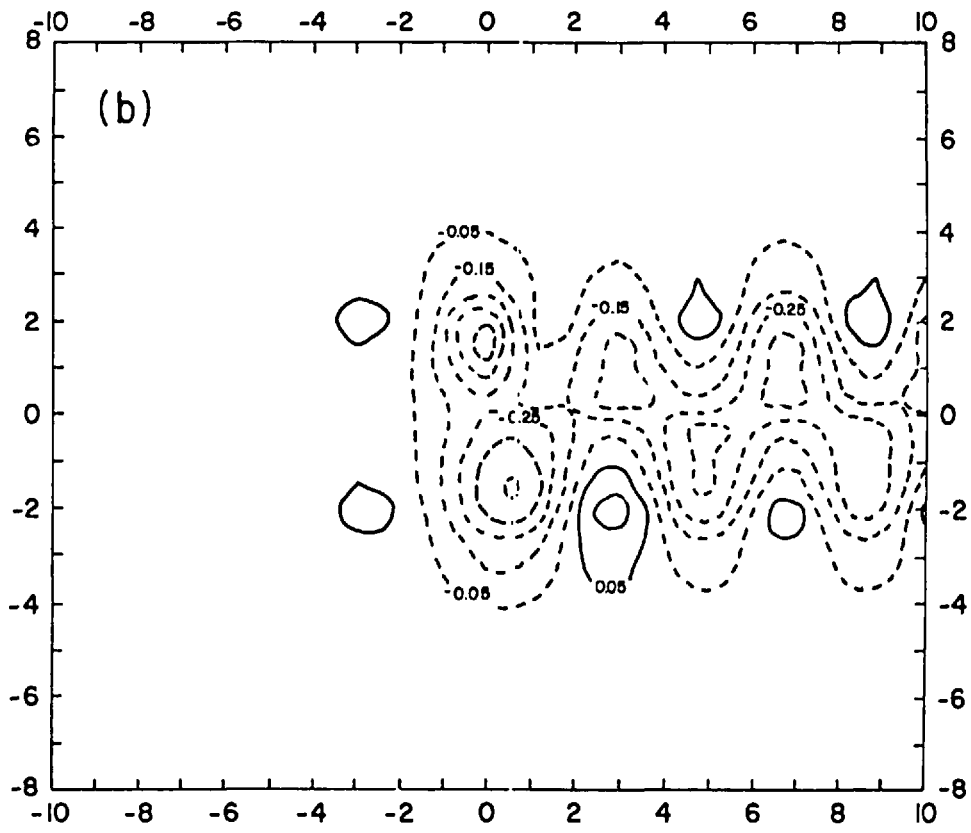

Figure 1b.

provided there is some amount of friction. Thus, G will be exponentially small as $|\mathbf{r}| \to \infty$, as mentioned in Section 3.

Asymptotic expansions for $\mathbf{K}$, $\mathbf{J}$ and $\mathscr{D}$ which are analogous to (4.39) may be easily derived with the aid of (4.28)-(4.30) and (4.34). The results are

$$\mathbf{K}(\mathbf{r};\mathbf{r}') \sim \sum_{m=-2}^{M-1} \mathbf{k}_m + (\gamma/4\pi)\exp[i\gamma(x-x')]\sum_{k=0}^{\infty}(i\sigma)^k \cdot \sum_{\mu,\epsilon=\pm 1} S_{k+1}\left(\frac{\mu+\epsilon}{2}; x, x'; \epsilon y, \mu y'\right) \cdot [\sigma W_{1k}(\sigma\epsilon y, \sigma\mu y')\hat{\mathbf{x}} + i\mu W_{2k}(\sigma\epsilon y, \sigma\mu y')\hat{\mathbf{y}}],$$

$$\mathbf{J}(\mathbf{r};\mathbf{r}') \sim \sum_{m=-2}^{M-1} \mathbf{j}_m - (\gamma/4\pi)\exp[i\gamma(x-x')]\sum_{k=0}^{\infty}(i\sigma)^k \cdot \sum_{\mu,\epsilon=\pm 1} S_{k+1}\left(\frac{\mu+\epsilon}{2}; x, x'; \epsilon y, \mu y'\right) \cdot [\sigma W_{1k}(\sigma\mu y', \sigma\epsilon y)\hat{\mathbf{x}} - i\epsilon W_{2k}(\sigma\mu y', \sigma\epsilon y)\hat{\mathbf{y}}],$$

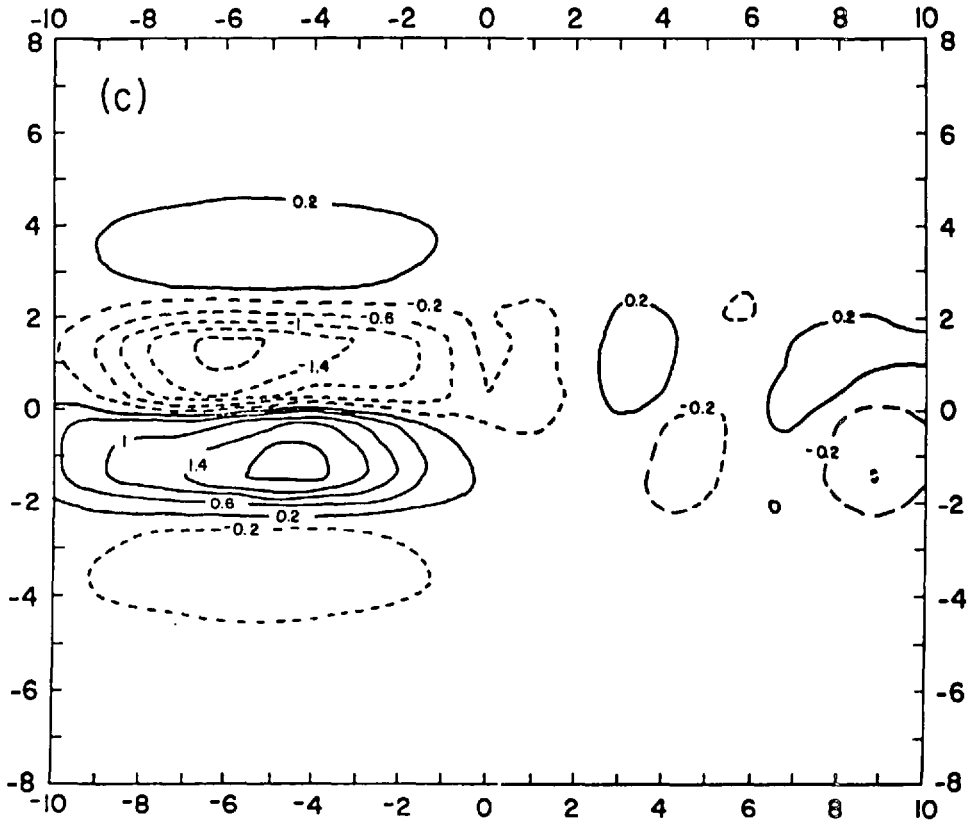

Figure 1c.

$$\mathscr{D}(\mathbf{r};\mathbf{r}') \sim \sum_{m=-2}^{M-1} \mathscr{A}_m + (\gamma/4\pi i)\exp\left[i\gamma(x-x')\right]\sum_{k=0}^{\infty}(i\sigma)^k$$

$$\cdot \sum_{\mu,\epsilon=\pm 1} S_k\left(\frac{\mu+\epsilon}{2}; x, x'; \epsilon y, \mu y'\right)$$

$$\cdot [W_{3k}(\sigma\epsilon y, \sigma\mu y')\hat{\mathbf{x}}\hat{\mathbf{x}} + i\sigma\mu W_{4k}(\sigma\epsilon y, \sigma\mu y')\hat{\mathbf{x}}\hat{\mathbf{y}}$$

$$- i\sigma\epsilon W_{4k}(\sigma\mu y', \sigma\epsilon y)\hat{\mathbf{y}}\hat{\mathbf{x}} + \epsilon\mu W_{5k}(\sigma\epsilon y, \sigma\mu y')\hat{\mathbf{y}}\hat{\mathbf{y}}], \qquad (4.47)$$

where $\mathbf{k}_m, \mathbf{j}_m, \mathscr{A}_m$ have their obvious meanings and

$$W_{1k}(y,y') = \sum_{n=0}^{k}\eta_{k-n}\sum_{j=0}^{n}A_j(y)B_{n-j}(y'),$$

$$W_{2k}(y,y') = \sum_{n=0}^{k}\eta_{k-n}\sum_{j=0}^{n}A_j(y)C_{n-j}(y'),$$

$$W_{3k}(y,y') = \sum_{n=0}^{k}\eta_{k-n}\sum_{j=0}^{n}B_j(y)B_{n-j}(y'),$$

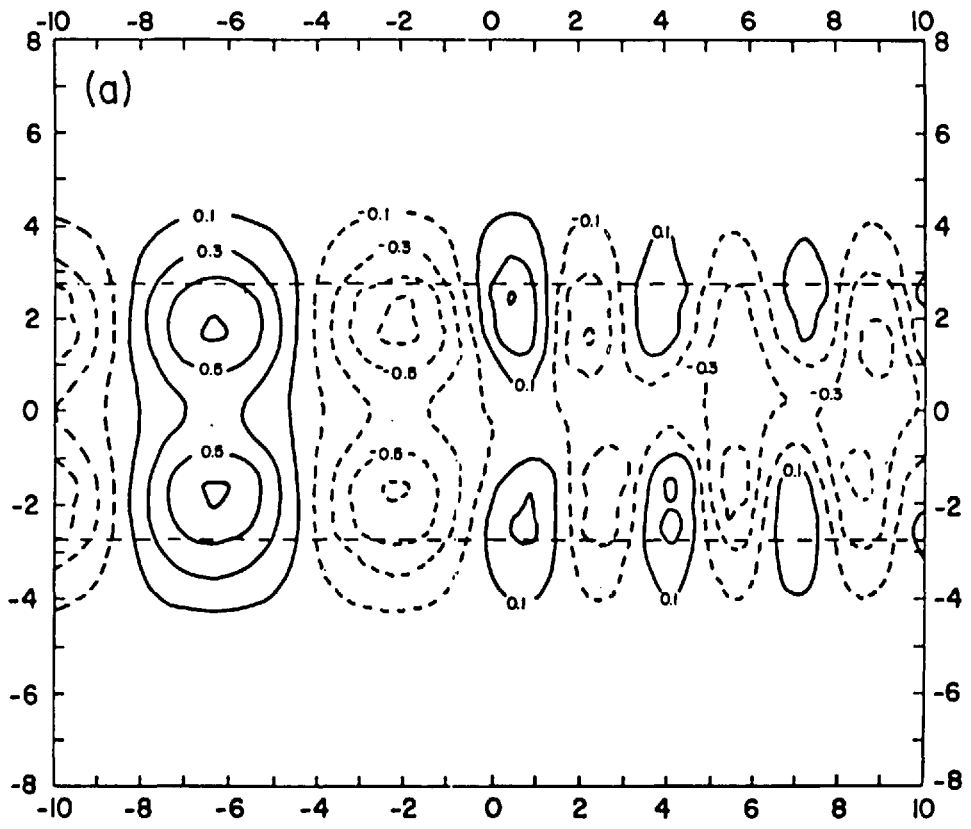

Figure 2. The same as Figure 1, but for a fixed non-dimensional frequency $y_c = 0.368$ and different meridional positions of the source. The "extreme latitudes" (see Section 4b) $y = \pm 2Q^{1/2} = \pm(y_c^2 + y_c^{-2})^{1/2} = \pm 2.739$ are identified by dashed lines. (a) Source at $\mathbf{r}' = (0, 0.5)$, between the extreme latitudes, radiating waves both to the east and to the west, as in Figure 1a. (b) Source at $\mathbf{r}' = (0, 2.739)$, on an extreme latitude, with an amplitude maximum around the source's position. (c) Source at $\mathbf{r}' = (0, 5)$, outside the extreme latitudes; no waves are radiated, and a local field build-up is observed within a deformation radius from the source.

$$W_{4k}(y, y') = \sum_{n=0}^{k} \eta_{k-n} \sum_{j=0}^{n} B_j(y) C_{n-j}(y'),$$

$$W_{5k}(y, y') = \sum_{n=0}^{k} \eta_{k-n} \sum_{j=0}^{n} C_j(y) C_{n-j}(y'). \tag{4.48}$$

We note that in (4.47) the expansions for $\mathbf{K}$, $\mathbf{J}$ and $\mathscr{D}$ involve the series $S_k(\nu; x, x'; y, y')$ for $k = 0, 1$, which diverge when $x = x'$; nevertheless, even in this case the expansions (4.47), (4.42) and (4.43) give meaningful results (Holvorcem, 1992).

c. Near-field behavior of the kernels. When $\mathbf{r}' \to \mathbf{r}$, the Green's function and the kernel functions become infinite. This singularity arises because the series $S_k(0; x, x'$;

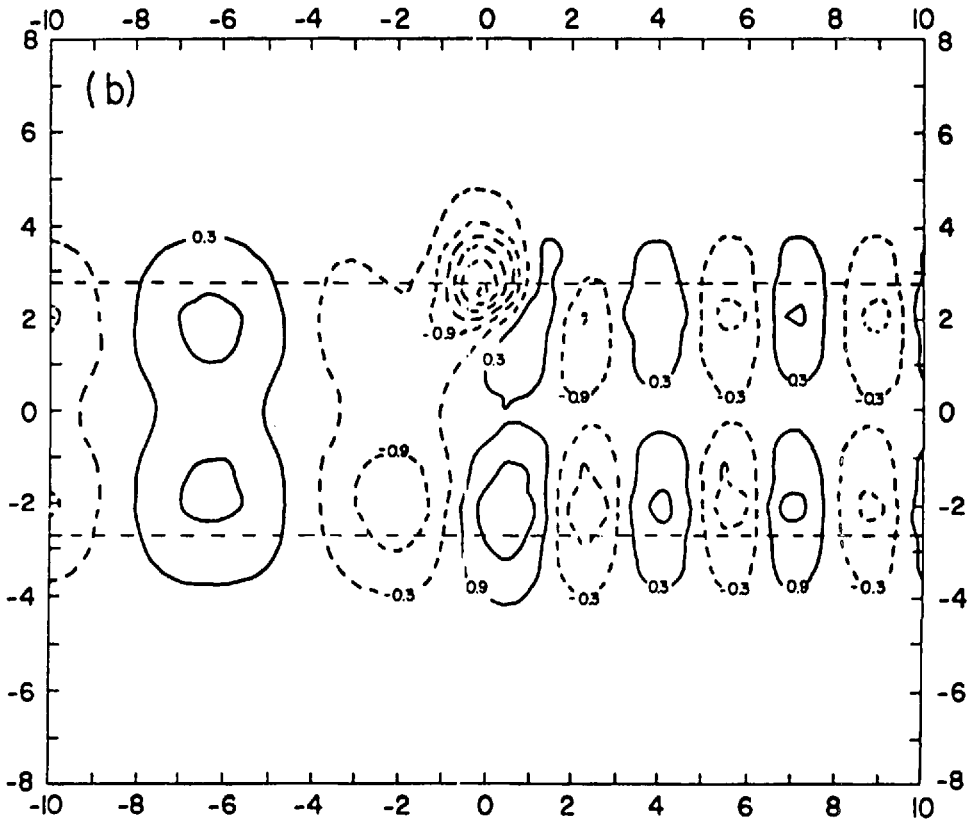

Figure 2b.

$\epsilon y, -\epsilon y')$ with $k = 0, 1, 2$, which appear in (4.39) and (4.47), have a singularity at $\mathbf{r}' = \mathbf{r}$, while the $S_k(\pm 1; x, x'; y, y')$ with $k = 0, 1, 2$ and $S_k(\nu; x, x'; y, y')$ with $k \geq 3$ are bounded functions of $\mathbf{r}$ and $\mathbf{r}'$ (see (4.42), (4.43) and the Appendix). Thus, the singularity is an effect of the superposition of damped equatorial modes. It is shown in the Appendix that when $\mathbf{r}' \to \mathbf{r}$ the $S_k(0; x, x'; \epsilon y, -\epsilon y')$ with $k = 0, 1, 2$ behave as $2[\xi_o(x, x'; \epsilon y, -\epsilon y')]^{-2}$, $2[\xi_o(x, x'; \epsilon y, -\epsilon y')]^{-1}$ and $-2 \ln \xi_o(x x'; \epsilon y, -\epsilon y')$, respectively. Expanding the coefficients of $S_k(0; x, x'; \epsilon y, -\epsilon y')$ in (4.39) and (4.47) in powers of $(x - x')$ and $(y - y')$, we may then show that the Green's function and the kernels have the following singular behavior as $\mathbf{r}' \to \mathbf{r}$:

$$G(\mathbf{r}; \mathbf{r}') \sim i(\gamma/\pi)(y^2 - y_c^2) \ln R + O(1), \tag{4.49}$$

$$\mathbf{K}(\mathbf{r}; \mathbf{r}') \sim (\gamma/2\pi)\{-2(y_c - iy\hat{\mathbf{z}} \times)(\mathbf{R}/R^2) + (i\hat{\mathbf{x}} - 2\gamma y\hat{\mathbf{y}}) \ln R\} + O(1), \tag{4.50}$$

$$\mathbf{J}(\mathbf{r}; \mathbf{r}') \sim (\gamma/2\pi)\{2(y_c + iy\hat{\mathbf{z}} \times)(\mathbf{R}/R^2) - (i\hat{\mathbf{x}} + 2\gamma y\hat{\mathbf{y}}) \ln R\} + O(1), \tag{4.51}$$

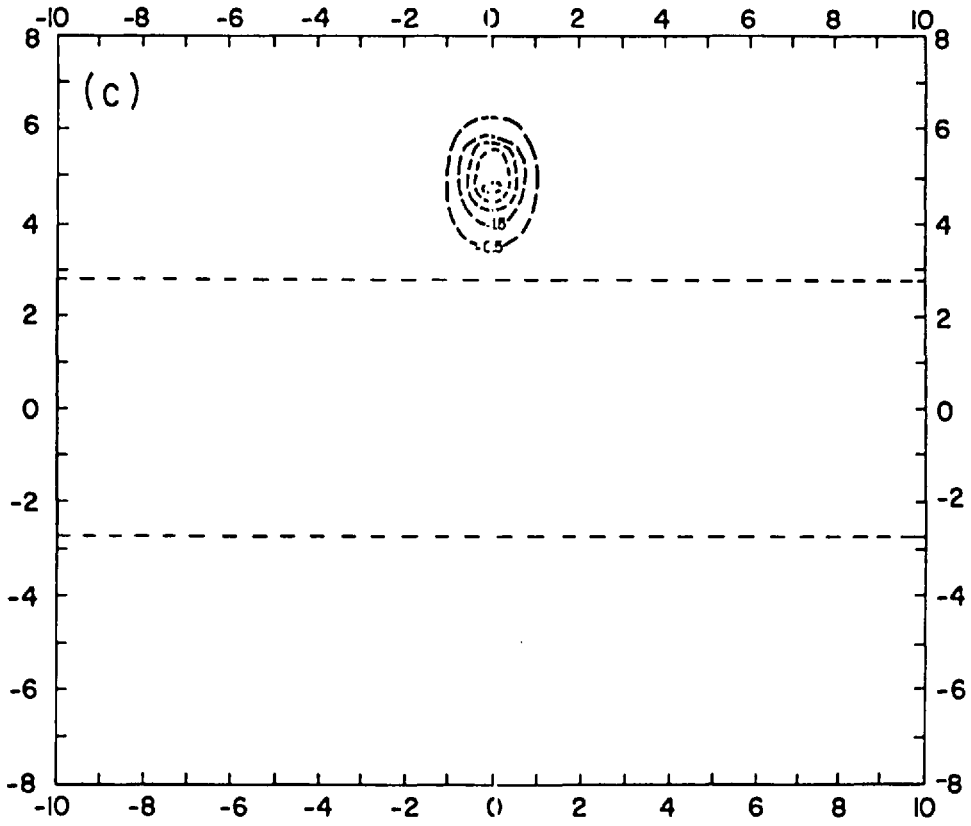

Figure 2c.

$$\begin{aligned}\mathscr{D}(\mathbf{r};\mathbf{r}') \sim\ & (\gamma/4\pi i)\big[4(1+i\gamma\Delta x)(\Delta x^2-\Delta y^2)R^{-4}(\hat{\mathbf{x}}\hat{\mathbf{x}}-\hat{\mathbf{y}}\hat{\mathbf{y}}) \\ & + 4\Delta y[2\Delta x + i\gamma(\Delta x^2-\Delta y^2)]R^{-4}(\hat{\mathbf{x}}\hat{\mathbf{y}}+\hat{\mathbf{y}}\hat{\mathbf{x}}) + 8i\gamma\Delta x R^{-2}\hat{\mathbf{y}}\hat{\mathbf{y}} \\ & + [(\tfrac{1}{2})(y^2+y_c^2)(\hat{\mathbf{x}}\hat{\mathbf{x}}+\hat{\mathbf{y}}\hat{\mathbf{y}}) - 2\gamma^2(\hat{\mathbf{x}}\hat{\mathbf{x}}+3\hat{\mathbf{y}}\hat{\mathbf{y}}) \\ & - iy_c y(\hat{\mathbf{x}}\hat{\mathbf{y}}-\hat{\mathbf{y}}\hat{\mathbf{x}})]\ln R\big] + \mathrm{O}(1).\end{aligned} \tag{4.52}$$

In (4.49)–(4.52) we use the notations $\mathbf{R} = \mathbf{r} - \mathbf{r}' = \Delta x\hat{\mathbf{x}} + \Delta y\hat{\mathbf{y}}$ and $R = |\mathbf{R}|$.

5. Boundary integral equations

After the detailed study of the kernel functions, we are ready to derive the fundamental boundary integral equation (BIE) of our formulation from the integral representation (3.10) for the pressure field. This representation was obtained under the assumption that $\mathbf{r}'$ is an interior point of the ocean region B. Now, suppose that $\mathbf{r}'$ is at a position $s = s'$ on Γ. By (4.50), the first integrand in (3.10) behaves as $(s - s')^{-1}$ as $s \to s'$. Thus, the first integral in (3.10) will be undefined even as an improper

Riemann integral. In order to correctly interpret this integral, we consider a limit process, where $\mathbf{r}'$ approaches a point $\mathbf{r}''$ on Γ from the interior of B, along the normal direction $\hat{\mathbf{n}}(s'')$, where s'' is the coordinate of $\mathbf{r}''$ on Γ. Denote by $Z(\delta s)$ the contribution to the integral from a short segment $s'' - \delta s \le s \le s'' + \delta s$. If the distance δn between $\mathbf{r}'$ and $\mathbf{r}''$ is small, then by (4.50) we have

$$Z(\delta s) = -(\gamma/\pi)p(\mathbf{r}'') \int_{s''-\delta s}^{s''+\delta s} \hat{\mathbf{n}}(s'') \cdot (y_c - iy''\hat{\mathbf{z}} \times) \frac{[\mathbf{r}' - \mathbf{r}(s)]}{|\mathbf{r}' - \mathbf{r}(s)|^2} ds + O(\delta s). \quad (5.1)$$

Since $\mathbf{r}(s) = \mathbf{r}'' + (s - s'')\hat{\mathbf{s}}(s'') + O((s - s'')^2)$ and $\mathbf{r}'' - \mathbf{r}' = \delta n \hat{\mathbf{n}}(s'')$, we conclude that

$$\begin{aligned} Z(\delta s) &= (\gamma/\pi)p(\mathbf{r}'') \int_{s''-\delta s}^{s''+\delta s} \frac{iy''(s - s'') + y_c \delta n}{\delta n^2 + (s - s'')^2} ds + O(\delta s) \\ &= \pi^{-1} p(\mathbf{r}'') \tan^{-1}(\delta s/\delta n) + O(\delta s). \end{aligned} \quad (5.2)$$

Taking the limit $\delta s, \delta n \to 0$ with $\delta n \ll \delta s$, we see that $Z(\delta s) \to p(\mathbf{r}'')/2$. Thus, when $\mathbf{r}'$ is at the position $s = s'$ on Γ, the first integral in (3.10) should be interpreted as

$$\frac{1}{2}p(\mathbf{r}') + \lim_{\delta s \to 0} \int_{|s-s'| \ge \delta s} p(\mathbf{r})\hat{\mathbf{n}}(s) \cdot \mathbf{K}(\mathbf{r}'; \mathbf{r})\, ds. \quad (5.3)$$

The second term in the above expression is called the "principal value" of the first integral in (3.10). By (4.49) and (4.50), the other integrals in (3.10) have integrable singularities at $\mathbf{r} = \mathbf{r}'$, so that no further interpretation is needed for them. Thus, the fundamental BIE for the boundary pressure distribution $p(s) = p(\mathbf{r}(s))$ is

$$\begin{aligned} \frac{1}{2}p(\mathbf{r}') = \text{P.V.} \oint_\Gamma p(\mathbf{r})\hat{\mathbf{n}}(s) \cdot \mathbf{K}(\mathbf{r}'; \mathbf{r})\, ds - \frac{1}{2}\rho_o c \oint_\Gamma q(s) G(\mathbf{r}'; \mathbf{r})\, ds \\ - \iint_B \mathbf{F}'(\mathbf{r}) \cdot \mathbf{K}(\mathbf{r}'; \mathbf{r})\, dx\, dy, \end{aligned} \quad (5.4)$$

where $\mathbf{r}'$ is at a position s' on Γ and P.V. denotes the principal value.

a. Boundary element method. Since the kernel functions are very complicated, it is difficult to solve (5.4) analytically, even if the basin geometry, the forcing and the boundary conditions are very simple. However, once we write a computer routine for the evaluation of the kernels using the analytic and asymptotic expressions of Section 4, the basic BIE (5.4) may be solved numerically by the standard Boundary Element Method (BEM) (Brebbia *et al.*, 1984). In this approach, we divide the boundary Γ into N short segments (boundary elements) $\Gamma_1, \ldots, \Gamma_N$. In each element Γ_j, we choose a point $\mathbf{r}_j'$, and assume that the pressure along each element is constant, equal to $p_j = p(\mathbf{r}_j')$. Applying (5.4) at $\mathbf{r}' = \mathbf{r}_k'$, $k = 1, \ldots, N$, we get a system of linear

equations for the boundary pressures p_j:

$$\frac{1}{2}p_k = \sum_{j=1}^{N} T_{kj}p_j - Q_k, \tag{5.5}$$

where

$$T_{kj} = \int_{\Gamma_j} \hat{\mathbf{n}}(s) \cdot \mathbf{K}(\mathbf{r}'_k; \mathbf{r})\, ds \tag{5.6}$$

and

$$Q_k = \frac{1}{2}\rho_o c \sum_{n=1}^{N} \oint_{\Gamma_n} q(s)G(\mathbf{r}'_k; \mathbf{r})\, ds + \iint_B \mathbf{F}'(\mathbf{r}) \cdot \mathbf{K}(\mathbf{r}'_k; \mathbf{r})\, dx\, dy. \tag{5.7}$$

Very realistic ocean geometries can be described by, say, about 100 elements, so that the dimension N of the above system of equations will normally be quite modest.

The simplest scheme uses straight-line boundary elements. In this case, $T_{kj} = \hat{\mathbf{n}}_j \cdot \int_{\Gamma_j} \cdot\, \mathbf{K}(\mathbf{r}'_k; \mathbf{r})\, ds$. If $j \neq k$, the point $\mathbf{r}'_k$ is not on the path of integration in this last integral, so that a numerical quadrature rule may be used for the evaluation of T_{kj}. When $j = k$, there is a singularity in the integrand at $\mathbf{r} = \mathbf{r}'_k$, and as we have seen the integral should be regarded as a principal value integral. To evaluate numerically this integral, we may express $\mathbf{K}(\mathbf{r}'_k; \mathbf{r}) = \mathbf{K}^{(S)}(\mathbf{r}'_k; \mathbf{r}) + \mathbf{K}^{(R)}(\mathbf{r}'_k; \mathbf{r})$, where $\mathbf{K}^{(S)}$ consists of the singular contributions given by (4.50) and $\mathbf{K}^{(R)}$ represents the O(1) "regular part" of $\mathbf{K}$. (Note that we may compute $\mathbf{K}^{(R)}$ using (4.50) and a computer routine which evaluates $\mathbf{K}$, by writing $\mathbf{K}^{(R)} = \mathbf{K} - \mathbf{K}^{(S)}$.) The principal value of $\int_{\Gamma_k} \mathbf{K}^{(S)}(\mathbf{r}'_k; \mathbf{r})\, ds$ is easily evaluated analytically, and $\int_{\Gamma_k} \mathbf{K}^{(R)}(\mathbf{r}'_k; \mathbf{r})\, ds$ may be computed by numerical quadrature. A similar approach may be used for the computation of the boundary integrals in (5.7), whose integrand has a singularity when $n = k$. This splitting of the kernels into singular and regular parts for purposes of numerical integration is commonly employed in the boundary element method (see, e.g., Dawson and Fawcett, 1990; Vijayakumar and Cormack, 1988).

b. Domain integrals. Although (5.4) is an equation for the function $p(s)$ of the single variable s, the presence of a domain integral as a forcing term seems to imply that a numerical code for the solution of (5.4) must involve the discretization of the basin B into small cells for purposes of numerical quadrature. However, the domain integral term may be replaced by a boundary integral by the use of particular solutions (Azevedo and Brebbia, 1988). For example, suppose that we want to solve the shallow water equations over an ocean basin B, with slip boundary conditions at the boundaries and a forcing field $\mathbf{F}(\mathbf{r})$. If we have a particular solution $p^{(P)}(\mathbf{r})$ of (2.7) (which in general will not satisfy the boundary conditions), then the total perturba-

tion pressure field may be written as

$$p = p^{(P)} + p^{(H)}, \tag{5.8}$$

where $p^{(H)}$ satisfies the homogeneous shallow water equations. At interior points $\mathbf{r}'$, the field $p^{(H)}$ may be represented, using identity (3.2), as

$$p^{(H)}(\mathbf{r}') = \oint_\Gamma p^{(H)}(\mathbf{r})\hat{\mathbf{n}}(s) \cdot \mathbf{K}(\mathbf{r}'; \mathbf{r})\, ds + \frac{1}{2}\rho_o c \oint_\Gamma G(\mathbf{r}'; \mathbf{r})\mathbf{u}^{(P)}(\mathbf{r}) \cdot \hat{\mathbf{n}}(s)\, ds, \tag{5.9}$$

where $\mathbf{u}^{(P)}$ denotes the velocity field associated with the particular solution $p^{(P)}$. When $\mathbf{r}'$ is taken to the boundary, we obtain a BIE for the unknown field $p^{(H)}$ which is analogous to (5.4), but without the domain integral term and with $-\mathbf{u}^{(P)} \cdot \hat{\mathbf{n}}$ playing the role of q. This BIE will involve only boundary integrals, and could be solved numerically by a boundary element scheme similar to (5.5)–(5.7).

To construct a particular solution for the pressure, associated with a realistic wind stress distribution, one may begin by calculating the response of an unbounded β-plane ocean to some class of "simple" wind stress distributions. If the realistic forcing field can be expanded as a linear combination of these "simple" distributions, then the sought for particular solution is given by the same linear combination of the calculated unbounded ocean responses.

A wind stress distribution which is sinusoidal in x and y is probably the most advantageous choice to compute the unbounded ocean response, since it allows the response to be determined analytically and since the decomposition of a realistic forcing field into its Fourier components is efficiently performed by FFT algorithms. Thus, it is sufficient to calculate the response to a forcing of the form

$$\mathbf{F}(\mathbf{r}) = \mathbf{F}_o \exp\,[i(ax + by)] \tag{5.10}$$

where a, b and $\mathbf{F}_o$ are constants. A particular pressure field driven by (5.10) is obtained from (3.10) by taking the region B as the whole plane,

$$p^{(P)}(\mathbf{r}) = -\mathbf{F}_o' \cdot \int_{-\infty}^{\infty}\int_{-\infty}^{\infty} \exp\,[i(ax' + by')]\mathbf{K}(\mathbf{r}; \mathbf{r}')\, dx'\, dy', \tag{5.11}$$

where $\mathbf{F}_o' = R_o\mathbf{F}_o$. Inserting the meridional mode expansion of $\mathbf{K}$, given by (4.22), and using the well-known property

$$\int_{-\infty}^{\infty} e^{iby}\psi_m(y/\sqrt{2})\, dy = 2\sqrt{\pi}i^m\psi_m(\sqrt{2}b), \tag{5.12}$$

one can rewrite (5.11) as

$$p^{(P)}(\mathbf{r}) = e^{iax}\mathbf{P}(a, b; y) \cdot \mathbf{F}_o', \tag{5.13}$$

where

$$\begin{aligned}\mathbf{P}(a,b;y) = -i(\pi/2)^{1/2}\Big\{&(a+\alpha_{-2})^{-1}\psi_o(y/\sqrt{2})\psi_o(\sqrt{2}b)\hat{\mathbf{x}}\\&+ i(a+\alpha_{-1})^{-1}\psi_1(y/\sqrt{2})[\psi_1(\sqrt{2}b)\hat{\mathbf{x}} - 4\gamma\psi_o(\sqrt{2}b)\hat{\mathbf{y}}]\\&- \gamma\sum_{\sigma=\pm1}\sigma\sum_{m=0}^{\infty}\frac{i^m\phi_m^\sigma(y)[\phi_m^\sigma(2b)\hat{\mathbf{x}} + 2\theta_m^\sigma(2b)\hat{\mathbf{y}}]}{\lambda_m(\sigma\lambda_m-\lambda_{-1})(\sigma\lambda_m-\lambda_{-2})(a+\sigma\lambda_m-\gamma)}\Big\}.\end{aligned} \tag{5.14}$$

The corresponding velocity field may analogously be obtained from (3.12), (4.24) and (5.12). The result is

$$\begin{aligned}\mathbf{u}^{(P)}(\mathbf{r}) = (\rho_o\omega_o)^{-1}\big\{&\exp[i(ax+by)](y^2-y_c^2)^{-1}(iy_c - y\hat{\mathbf{z}}\times)\mathbf{F}_o\\&+ e^{iax}\mathscr{U}(a,b;y)\cdot\mathbf{F}_o\big\},\end{aligned} \tag{5.15}$$

where $\omega_o = \beta R_o$ and

$$\begin{aligned}\mathscr{U}(a,b;y) = -i(\pi/8)^{1/2}\Big\{&(a+\alpha_{-2})^{-1}\psi_o(y/\sqrt{2})\psi_o(\sqrt{2}b)\hat{\mathbf{x}}\hat{\mathbf{x}}\\&+ i(a+\alpha_{-1})^{-1}[\psi_1(y/\sqrt{2})\hat{\mathbf{x}} + 4i\gamma\psi_o(y/\sqrt{2})\hat{\mathbf{y}}][\psi_1(\sqrt{2}b)\hat{\mathbf{x}} - 4\gamma\psi_o(\sqrt{2}b)\hat{\mathbf{y}}]\\&- 2\gamma\sum_{\sigma=\pm1}\sigma\sum_{m=0}^{\infty}\frac{i^m[\zeta_m^\sigma(y)\hat{\mathbf{x}} - i\theta_m^\sigma(y)\hat{\mathbf{y}}][\phi_m^\sigma(2b)\hat{\mathbf{x}} + 2\theta_m^\sigma(2b)\hat{\mathbf{y}}]}{\lambda_m(\sigma\lambda_m-\lambda_{-1})(\sigma\lambda_m-\lambda_{-2})(a+\sigma\lambda_m-\gamma)}\Big\}.\end{aligned} \tag{5.16}$$

In trying to evaluate numerically a particular solution using series (5.14) and (5.16) directly, it is found that the first of these series converges very slowly, while the second diverges. In fact, a simple estimate using (4.12) and (4.28)–(4.30) shows that the general terms of (5.14) and (5.16) are $O(m^{-1})$ and $O(m^{-1/2})$, respectively, as $m \to \infty$. Due to the similarity between the particular solution series and the meridional mode expansions for the kernels of the BIEs, one can proceed as in Section 4b to derive rapidly convergent asymptotic expansions for the remainders of (5.14) and (5.16). Omitting the details of this calculation, the results may be written as

$$\begin{aligned}\mathbf{P}(a,b;y) = \mathbf{p}_{-2} + \mathbf{p}_{-1} + \sum_{m=0}^{M-1}\sum_{\sigma=\pm1}\mathbf{p}_m^\sigma\\- (\gamma/4\pi^{1/2})\sum_{k=0}^{\infty} i^k \sum_{\mu,\epsilon=\pm1}\\\cdot[iS'_{k+3}(\epsilon\mu;\mu b,\epsilon y)U_{1k}(a,\mu b;\epsilon y)\hat{\mathbf{x}}\\+ \mu S'_{k+2}(\epsilon\mu;\mu b;\epsilon y)U_{2k}(a,\mu b;\epsilon y)\hat{\mathbf{y}}],\end{aligned} \tag{5.17}$$

$$\begin{aligned}\mathscr{U}(a,b;y) = \mathscr{u}_{-2} + \mathscr{u}_{-1} + \sum_{m=0}^{M-1}\sum_{\sigma=\pm1}\mathscr{u}_m^\sigma\\+ (\gamma/4\pi^{1/2})\sum_{k=0}^{\infty} i^k \sum_{\mu,\epsilon=\pm1}\\\cdot\{\epsilon S'_{k+2}(\epsilon\mu;\mu b,\epsilon y)[\epsilon U_{3K}(a,\mu b;\epsilon y)\hat{\mathbf{x}}\hat{\mathbf{x}}\\+ iU_{4k}(a,\mu b;\epsilon y)\hat{\mathbf{y}}\hat{\mathbf{x}}] + \mu S'_{k+1}(\epsilon\mu;\mu b,\epsilon y)[iU_{5k}(a,\mu b;\epsilon y)\hat{\mathbf{x}}\hat{\mathbf{y}}\\+ \epsilon U_{6k}(a,\mu b;\epsilon y)\hat{\mathbf{y}}\hat{\mathbf{y}}]\},\end{aligned} \tag{5.18}$$

where $\mathbf{p}_{-2}$, $\mathbf{p}_{-1}$, α_{-2}, α_{-1} denote the terms of (5.14) and (5.16) corresponding to the Kelvin and Yanai waves, $\mathbf{p}_m^\sigma$ and α_m^σ are the general terms of those series, S'_k is the series

$$S'_k(\nu; b, y) = \sum_{m=M}^{\infty} i^{-\nu m} \tilde{m}^{-k/2} \exp\{-i[\chi(\tilde{m}, y) + \chi(\tilde{m}, 2b)]\}, \tag{5.19}$$

and the first coefficients $U_{nk} = U_{nk}(a, b; y)$ are given by

$$\begin{aligned}
&U_{10}(a,b;y) = 2(y_c^2 + 2by), \qquad U_{11}(a,b;y) = 2(ay_c - 1)(2b + y),\\
&U_{12}(a,b;y) = -(1/8)[y_c^2(4y_c^2 - 4b^2 - y^2) - 16(1 - ay_c)^2 +\\
&\qquad + 2by(32\gamma a(1 - ay_c) + y^2 + 4b^2)],\\
&U_{20}(a,b;y) = -4y_c, \qquad U_{21}(a,b;y) = -4ay,\\
&U_{22}(a,b;y) = (1/4)[16a(1 - ay_c) + y_c(4b^2 - y^2 + 4y_c^2)],\\
&U_{30}(a,b;y) = 4b, \qquad U_{31}(a,b;y) = 2(ay_c - 1),\\
&U_{32}(a,b;y) = (1/4)[2y_c^2 y + b(y^2 - 4b^2 - 32\gamma a(1 - ay_c))],\\
&U_{40}(a,b;y) = -2y_c, \qquad U_{41}(a,b;y) = -4ab,\\
&U_{42}(a,b;y) = (1/8)[16a(1 - ay_c) + y_c(4y_c^2 + y^2 - 4b^2)],\\
&U_{50}(a,b;y) = 0, \qquad U_{51}(a,b;y) = 4a, \qquad U_{52}(a,b;y) = y_c y,\\
&U_{60}(a,b;y) = 4, \qquad U_{61}(a,b;y) = 0,\\
&U_{62}(a,b;y) = -(1/4)(y^2 + 4y_c^2 + 4b^2 - 16a^2).
\end{aligned} \tag{5.20}$$

The expansions (5.17) and (5.18) are valid provided

$$M \gg 1, a^2, b^2, y^2/4, |Q|. \tag{5.21}$$

In this limit, the series $S'_k(\nu; b, y)$ may be asymptotically evaluated as (Holvorcem, 1992)

$$\begin{aligned}
S'_k(\nu; b, y) \sim\ & 2^{-1}\tilde{M}^{-k/2} i^{-\nu M} \exp\{-i[\chi(\tilde{M}, y) + \chi(\tilde{M}, 2b)]\}\\
&\cdot\{(1 - i\nu) + \tfrac{1}{2}i(y + 2b)\tilde{M}^{-1/2} + \tfrac{1}{8}[4k - i\nu(y + 2b)^2]\tilde{M}^{-1}\\
&- \tfrac{1}{16}[2\nu(2k + 1)(y + 2b) - i(y^3 + 4by^2 + 8b^2y + 8b^3)]\tilde{M}^{-3/2} + \cdots\}.
\end{aligned} \tag{5.22}$$

c. Computation of the interior fields. Once the homogeneous solution $p^{(H)}$ is numerically found at each boundary element, the solution at any interior point can be obtained from the integral representations (5.9) and

$$\mathbf{u}^{(H)}(\mathbf{r}') = -(2/\rho_o c) \oint_\Gamma p^{(H)}(\mathbf{r}) \mathscr{D}(\mathbf{r}'; \mathbf{r}) \cdot \hat{\mathbf{n}}(s)\, ds + \oint_\Gamma [\mathbf{u}^{(P)}(\mathbf{r}) \cdot \hat{\mathbf{n}}(s)] \mathbf{J}(\mathbf{r}'; \mathbf{r})\, ds, \tag{5.23}$$

which is an unforced version of (3.12). All the integrals in (5.9) and (5.23) can be numerically evaluated as sums of integrals over the boundary elements $\Gamma_1, \ldots \Gamma_N$.

Even though such integrals are non-singular (since $\mathbf{r}'$ does not lie on Γ), when the distance from $\mathbf{r}'$ to the boundary is less than one or two deformation radii the integrands in (5.9) and (5.23) will change rapidly over the elements which are closest to $\mathbf{r}'$, reflecting the singular behavior of the kernels as $\mathbf{r}' \to \mathbf{r}$. The most efficient procedure to evaluate each of these integrals is then to employ the splitting procedure already discussed at the end of Section 5a, that is, to integrate analytically the singular parts of the kernels (Eqs. (4.49)–(4.52)) and to use an ordinary numerical quadrature rule for their regular parts. This procedure is better than to compute the whole integral by a higher-order quadrature rule, since any such rule would become inaccurate for $\mathbf{r}'$ close enough to the boundary Γ (Section 4 of Part II of this series gives more details on the procedure).

6. Conclusion

Our ultimate objective is to build a linear time-dependent three-dimensional tropical ocean circulation model consisting of the usual superposition of vertical modes, including the effects of reflected equatorial waves from realistic basin boundary geometries. To accomplish this objective in a rigorous way, the first step consists of treating effectively the horizontal structure problem for each baroclinic mode, incorporating exact boundary conditions at irregular ocean boundaries. It is also known that several important aspects of equatorial ocean dynamics can be well described by the use of shallow water, single baroclinic mode reduced gravity models with realistic ocean boundaries (Busalacchi and Picaut, 1983) or realistically modeled wind-forcing fields (Weisberg and Tang, 1987, 1990).

The theory presented here shows how one can effectively use meridional mode expansions to describe the superposition of forced and reflected equatorial waves from arbitrary boundaries, by use of an analytical-numerical method which works even with negligible dissipation. The whole physics of the ocean circulation problem is contained in the kernel functions G, $\mathbf{K}$, $\mathbf{J}$ and $\mathscr{D}$ (Sections 3 and 4), which describe how the dynamical influences are propagated on an equatorial β-plane. The accurate evaluation of these functions has been accomplished by the use of asymptotic techniques for the summation of Hermite series. Such techniques are general in character, and are suitable for the treatment of most slowly converging (or even diverging) Hermite series which occur in equatorial oceanography (Holvorcem, 1992).

The present method deals in a clean, explicit way, with the short and zonally damped equatorial wave modes. These become important near ocean boundaries, but are often parameterized or neglected in the literature, by considering only low-frequency motions or invoking the long-wave approximation (Cane and Sarachik, 1981; Cane and Gent, 1984). The neglect of the short wave modes is usually justified by the effects of friction. In our model, we can vary the friction coefficient A and observe its effects on the solutions without having to neglect any mode right from the beginning.

The projection of the forcing field onto Fourier components (Section 5) and the asymptotic treatment of exact particular solutions effectively remove the computational difficulties pointed out by Cane and Patton (1984), concerning the use of normal mode decompositions and projections onto Hermite functions (or even parabolic cylinder functions of arbitrary order). In the present approach, all meridional mode expansions have known coefficients, and may be economically evaluated by explicit asymptotic formulas.

From the numerical viewpoint, an interesting feature of the boundary element method is the possibility of studying selected areas of the ocean at high resolution, ignoring completely what happens in the rest of the basin. Since integration is a smoothing process, the interior fields generated from (5.9) and (5.23) will generally be smoother than, say, a finite-difference solution. Besides, it is characteristic of the BEM that the resolution of the interior solution tends to be greater than the characteristic size of the boundary elements. This is in contrast to finite-difference/finite element schemes, where the resolution is of the order of the size of the grid cells.

Finally, it may be remarked that the integral representations (3.10) and (3.12) for the pressure and velocity fields could be helpful in the conception of a tropical ocean monitoring system, since they allow the explicit computation of the forced ocean motion from the wind-stress field and the coastal sea-level anomalies. A similar, but less general approach has been employed by Gill (1983) to reconstruct the field of anomalous motion in the tropical Pacific during the 1972 El Niño from time series of seal level anomaly at the eastern boundary.

Acknowledgments. We are grateful to Admiral Fernando Freitas and Admiral Maximiano da Fonseca, from the Diretoria de Transportes, and to Dr. Milton Francke, superintendent of DEPEX, all from PETROBRÁS, for their encouragement and for the support that made this research possible. One of us (P.R.H.) was supported by a PETROBRÁS fellowship, under grant SEDES-30239/89.

APPENDIX

Computation of the integral (4.46)

Here we present a method for the numerical evaluation of the integral defined in (4.46). With the change of variable $z = \tilde{m}^{1/2}$, the integral becomes

$$I_k(x, x'; y, y') = 2 \int_{z_o}^{\infty} z^{1-k} \exp\left[-\Phi(z^2; x, x'; y, y')\right] dz, \tag{A.1}$$

where $z_o = \tilde{M}^{1/2}$. If the quantity

$$\Lambda = z_o[(x - x')^2 + (y + y')^2]^{1/2} \tag{A.2}$$

is large enough, we can compute I_k from the asymptotic expansion (Holvorcem, 1992)

$$I_k(x,x';y,y') \sim 2\exp(-z_0\xi_0) \cdot \sum_{n=0}^{\infty} \xi_0^{-n-1} \frac{\partial^n}{\partial z^n} z^{1-k} \exp[-\Phi(z^2;x,x';y,y') + \xi_o z]|_{z=z_0}, \quad \text{(A.3)}$$

which is obtained from (A.1) by iterated integration by parts (Olver, 1974). In (A.3), $\xi_0 = \xi_0(x,x';y,y')$ is defined by (4.45). On the other hand, for bounded values of Λ we have the convergent expansion (Holvorcem, 1992)

$$I_k(x,x';y,y') = 2\sum_{n=0}^{\infty} q_n \xi_o^{n+k-2} \Gamma(2-n-k, z_o\xi_o), \quad \text{(A.4)}$$

where $\Gamma(n,z)$ denotes the incomplete gamma function (Abramowitz and Stegun, 1965) and the $q_n = q_n(x,x';y,y')$ are defined by the expansion

$$\exp[-\Phi(z^2;x,x';y,y') + \xi_o z] = \sum_{n=0}^{\infty} q_n z^{-n}. \quad \text{(A.5)}$$

In view of (4.44), we can express the q_n in terms of the ξ_n; the first coefficients are clearly given by

$$q_0 = 1, \qquad q_1 = -\xi_1, \qquad q_2 = \xi_1^2/2, \qquad q_3 = -\xi_2 - \xi_1^3/6. \quad \text{(A.6)}$$

To use (A.4) numerically, it is necessary to compute $\Gamma(n,z)$ for integer values of n. It is known that $\Gamma(n,z)$, $n = 1, 2, \ldots$, can be expressed in terms of elementary functions. When $n = 0$, we have $\Gamma(0,z) = E_1(z)$, the exponential integral (Abramowitz and Stegun, 1965), which may be computed from the truncated power series

$$E_1(z) \simeq -\ln z - 0.5772157 - \sum_{n=1}^{5} \frac{(-z)^n}{(n!)n} \quad \text{(A.7)}$$

for $|z| < 0.4$, and from the truncated continued fraction

$$E_1(z) \simeq \frac{e^{-z}}{z+}\,\frac{1}{1+}\,\frac{1}{z+}\,\frac{2}{1+}\,\frac{2}{z+}\cdots\frac{30}{1+}\,\frac{30}{z} \quad \text{(A.8)}$$

for $|z| > 0.4$. Finally, $\Gamma(n,z)$, $n = -1, -2, \ldots$, can be obtained from $\Gamma(0,z)$ by recurrence:

$$\Gamma(n-1,z) = (n-1)^{-1}[\Gamma(n,z) - z^{n-1}e^{-z}]. \quad \text{(A.9)}$$

The asymptotic expansion (A.3) truncated at $n = 3$ and the series (A.4) truncated at $n = 10$ match with an error of a few percent when $\Lambda \simeq 25$. Thus, we may compute $I_k(x,x';y,y')$ from (A.3) for $\Lambda \geq 25$ and from (A.4) for $\Lambda \leq 25$ (Olver, 1974).

The series (A.4) may be used to determine the behavior of $S_k(0;x,x';\epsilon y, -\epsilon y')$

when $x \to x', y \to y'$. For example, if $k = 2$ we have, by (4.43), (A.4) and (A.7):

$$\begin{aligned} S_2(0; x, x'; \epsilon y, -\epsilon y') &\sim I_2(x, x'; \epsilon y, -\epsilon y') + O(1) \\ &\sim 2E_1(z_0\xi_0(x, x'; \epsilon y, -\epsilon y')) + O(1) \\ &\sim -2\ln \xi_0(x, x'; \epsilon y, -\epsilon y') + O(1). \end{aligned} \tag{A.10}$$

Analogously, it can be verified that

$$\begin{aligned} S_0(0; x, x'; \epsilon y, -\epsilon y') &\sim 2[\xi_0(x, x'; \epsilon y, -\epsilon y')]^{-2} + O(1), \\ S_1(0; x, x'; \epsilon y, -\epsilon y') &\sim 2[\xi_0(x, x'; \epsilon y, -\epsilon y')]^{-1} + O(1), \\ S_k(0; x, x'; \epsilon y, -\epsilon y') &\sim O(1), \qquad k = 3, 4, \ldots \end{aligned} \tag{A.11}$$

REFERENCES

Abramowitz, M. and I. Stegun. 1965. Handbook of Mathematical Functions, Dover, New York, 1046 pp.

Azevedo, J. P. S. and C. A. Brebbia. 1988. An efficient technique for reducing domain integrals to the boundary, *in* Boundary Elements X, *1,* C. A. Brebbia, ed., Computational Mechanics Publications, Southampton, 347–361.

Battisti, D. S. and A. C. Hirst. 1989. Interannual variability in a tropical ocean-atmosphere model: influence of the basic state, ocean geometry and nonlinearity. J. Atm. Sci., *46,* 1687–1712.

Boyd, J. P. and D. W. Moore. 1986. Summability methods for Hermite functions. Dyn. Atmos. Oceans, *10,* 51–62.

Brebbia, C. A., J. C. F. Telles and L. C. Wrobel. 1984. Boundary Element Techniques, Springer-Verlag, Berlin, 463 pp.

Bruce, J. G., J. L. Kerling and W. H. Beatty III. 1985. On the North Brazilian eddy field. Prog. Oceanogr., *14,* 57–63.

Bryan, K. 1969. A numerical method for the study of the circulation of the World Ocean. J. Comput. Phys., *4,* 347–376.

Busalacchi, A. J. and J. Picaut. 1983. Seasonal variability from a model of the tropical Atlantic Ocean. J. Phys. Oceanogr., *13,* 1564–1588.

Butkov, E. 1968. Mathematical Physics. Addison-Wesley, Reading, Massachusetts, 735 pp.

Cane, M. A. and P. R. Gent. 1984. Reflection of low-frequency equatorial waves at arbitrary western boundaries. J. Mar. Res., *42,* 487–502.

Cane, M. A. and R. J. Patton. 1984. A numerical model for low-frequency equatorial dynamics. J. Phys. Oceanogr., *14,* 1853–1863.

Cane, M. A. and E. S. Sarachik. 1981. The response of a linear baroclinic equatorial ocean to periodic forcing. J. Mar. Res., *39,* 651–693.

—— 1983. Equatorial Oceanography. Rev. Geophys. and Space Phys., *21,* 1137–1148.

Carton, J. A. 1989. Estimates of sea level in the tropical Atlantic ocean using Geosat altimetry. J. Geophys. Res., *94C,* 8029–8039.

Dawson, T. W. and J. A. Fawcett. 1990. A boundary integral equation method for acoustic scattering in a waveguide with nonplanar surfaces. J. Acoust. Soc. Am., *87,* 1110–1125.

du Penhoat, Y. and Y. Gouriou. 1987. Hindcast of equatorial sea surface dynamic height in the Atlantic in 1982–1984. J. Geophys. Res., *92C,* 3729–3740.

du Penhoat, Y. and A. M. Treguier. 1985. The seasonal linear response of the tropical Atlantic Ocean. J. Phys. Oceanogr., *15,* 316–329.

Friedman, B. 1956. Principles and Techniques of Applied Mathematics, John Wiley & Sons, New York, 315 pp.

Gill, A. E. 1983. An estimation of sea-level and surface-current anomalies during the 1972 El Niño and consequent thermal effects. J. Phys. Oceanogr., *13,* 586–606.

Hildebrand, F. B. 1965. Advanced Calculus for Applications. Prentice-Hall, Englewood Cliffs, New Jersey, 646 pp.

Holvorcem, P. R. 1992. Asymptotic summation of Hermite series. J. Phys. A: Math. Gen., (in press).

Holvorcem, P. R. and M. L. Vianna. 1992. Integral equation approach to tropical ocean dynamics. Part II—Rossby wave scattering from the equatorial Atlantic western boundary. J. Mar. Res., *50,* 33–63.

Jacobs, S. J. 1967. An asymptotic solution of the tidal equations. J. Fluid Mech., *30,* 417–438.

Longuet-Higgins, M. S. 1965. Planetary waves on a rotating sphere. II. Proc. Roy. Soc. London, Ser. A, *284,* 40–54.

Matsuno, T. 1966. Quasi-geostrophic motions in the equatorial area. J. Met. Soc. Japan, Ser. II, *44,* 25–43.

McCreary, J. P. 1981. A linear stratified ocean model of the equatorial undercurrent. Phil. Trans. Roy. Soc. London, Ser. A, *298,* 603–635.

—— 1985. Modeling equatorial ocean circulation. Ann. Rev. Fluid Mech., *17,* 359–409.

McCreary, J. P., J. Picaut and D. W. Moore. 1984. Effects of remote annual forcing in the eastern tropical Atlantic Ocean. J. Mar. Res., *42,* 45–81.

Olver, F. W. J. 1974. Asymptotics and Special Functions. Academic Press, New York, 572 pp.

Philander, S. G. H. and R. C. Pacanowski. 1986. A model of the seasonal cycle of the tropical Atlantic Ocean. J. Geophys. Res., *91C,* 212–214.

—— 1987. Nonlinear effects in the seasonal cycle of the tropical Atlantic Ocean. Deep-Sea Res., *34,* 123–137.

Picaut, J., J. Servain, P. Lecomte, M. Seva, S. Lukas and G. Rougier. 1985. Climatic atlas of the tropical Atlantic wind stress and sea surface temperature 1964–1979. Université de Bretagne Occidentale—University of Hawaii, 467 pp.

Ripa, P. 1989. Rays in the equatorial oceans. Tropical Ocean—Atmosphere Newsletter No. 48, 1–5.

Seager, R., S. E. Zebiak and M. A. Cane. 1988. A model of the tropical Pacific sea surface temperature climatology. J. Geophys. Res., *93C,* 1265–1280.

Vianna, M. L. 1988. Stratified tropical ocean dynamics: effects of coastal geometry on the linear response to wind by boundary integral equation formulation, *in* Boundary Elements X, *2,* C. A. Brebbia, ed., Computational Mechanics Publications, Southampton, 289–300.

Vijayakumar, S. and D. E. Cormack. 1988. An invariant imbedding method for singular integral evaluation on finite domains. SIAM J. Appl. Math., *48,* 1335–1349.

Weisberg, R. H. and T. Y. Tang. 1987. Further studies on the response of the equatorial thermocline in the Atlantic Ocean to the seasonally varying trade winds. J. Geophys. Res., *92C,* 3709–3727.

—— 1990. A linear analysis of equatorial Atlantic Ocean thermocline variability. J. Phys. Oceanogr., *20,* 1813–1825.

Zebiak, S. E. and M. A. Cane. 1987. A model El Niño-Southern Oscillation. Mon. Wea. Rev., *115,* 2262–2278.

Received: *9 May, 1990;* revised: *7 January, 1992.*